A THESIS

ON

STUDIES ON PERMEABILTY OF Mn-Zn SOFT FERRITES ON VARIATION IN ITS BASIC COMPOSITION

Submitted in partial fulfillment of the requirements for the award of the degree of

Master of Technology (M.Tech.)

IN

MATERIALS SCIENCE AND ENGINEERING

Submitted By

Ishwinder Pal singh

ROLL NO. 6050502

Under The Guidance Of

Dr.O.P. PANDEY

Professor and Head, SPMS

Thapar University, Patiala, Punjab (147004)

SCHOOL OF PHYSICS AND MATERIAL SCIENCES
THAPAR UNIVERSITY
PATIALA (PUNJAB)-147004, INDIA.

JUNE 2007.

CERTIFICATE

This is to certify that the thesis entitled, **"STUDIES ON PERMEABILTY OF Mn-Zn SOFT FERRITES ON VARIATION IN ITS BASIC COMPOSITION",** submitted by **Mr. Ishwinder Pal Singh** in the partial fulfillment of the requirement for the award of the degree of **M. Tech** in **Materials Science and Engineering** from the **School of Physics and Materials Science, Thapar University, Patiala,** is a record of candidate's own work carried out by him under our supervision and guidance. The matter embodied in this report has not been submitted in part or full to any other university or institute for the award of any degree.

.

(Dr. O.P.Pandey)

Professor and Head,

School of Physics and Materials Science

Thapar University,

Patiala, Punjab.

(Dr. R.K.Sharma)

Dean, Academic Affairs

Thapar University,

Patiala, Punjab (147004)

Dated:

ACKNOLEDGEMENT

Knowledge in itself is a continuous process. I would have never succeeded in completing my task without the cooperation, encouragement and help provided to me by various personalities.

With deep sense of gratitude I express my sincere thanks to my esteemed and worthy supervisor, **Dr. O. P. Pandey**, Professor and Head, School of Physics and Materials Science, for his valuable guidance in caring out this work under his effective supervision, encouragement and unforgettable cooperation.

I wish to express my sincere thanks to P.G. Incharge **Dr. Kulvir Singh,** assistant Professor School of Physics and Materials Science, who have been a constant source of inspiration for me throughout this project work.

I would also like to thank **Mr. K. Shriram** and **Mr. Sameer Yadav** , **Cosmo-ferrites ltd, Solan,** to provide me an opportunity to work in there premier R & D Department and opening all its facilities to me.

I am deeply thankful to my **Family,** especially my **Mother Mrs Gurmeet Kaur**, for all that they have done for me and for this, word 'thankful' is very small, and to My wife **Gazal**, who supported me with her time, I believe that their patience have beard fruit through completion of this Thesis which will result in award of the prestigious degree of M.Tech Materials science & Engineering.

I am also thankful to all the staff members of School of Physics and Materials Science, My friends **Vishal Kumar, Pankaj Kumar, Miss Anu Arora** and **Vajinder Singh**, for their full cooperation and help. The technical guidance and constant encouragement made it possible to tie over the numerous problems, which so ever came up during the study. My greatest thanks are to all who wished me success.

Above all I render my gratitude to the Almighty **Shri Guru Nanak Dev Ji**, who bestowed self –confidence, ability, strength and path to me in accomplishing this work.

Ishwinder Pal Singh

Roll no.- 6050502

ABSTRACT

In response to the current demand for size reduction of electronic devices, the development of compact and efficient switched-mode-power supplies has received considerable attention. Power supplies being an integral part of electronic equipments from computers and microprocessors to TV and video tape-recorders, the demand for ferrite cores, which are an essential component of the switching power supplies, is continuously on the rise.

This can be achieved by low loss, High Permeability Mn-Zn Ferrites. In the present work effort have been made to study permeability spectrum of Mn-Zn soft ferrite cores by variation in basic composition at a constant doping of Bi_2O_3. It was studied through this experimentation that how a wrong stociometric composition can lead to loss in permeability. It was found that for a composition Fe_2O_3 52.510 mol%, Mn_2O_3 24.390 mol%, ZnO 23.100 mol% and Bi_2O_3 0.02 wt % , out of prepared samples the permeability, showed its maximum in comparison with other prepared samples.

****

Dedicated To My

Parents

CONTENTS

Certificate

Acknowledgement

Abstract

Page

CHAPTER- 1 1-5

Introduction

CHAPTER- 2 LITERATURE SURVEY 6-43

2.1 Crystal Structures of Ferrites 7

2.1.1 Classes of Crystal structures in ferrites 7

1. Spinal structure 8
2. Hexagonal Ferrites 11
3. Magnetic rare earth garnets 12

2.2 The Magnetization in Domains and Bulk Materials 13

2.2. 1. The nature of domains 13

1. Magnetostatic Energy 14
2. Magnetocrystalline Anisotropy Energy 15
3. Magnetostrictive Energy 16
4. Domain Wall Energy 17

2.2.2. Proof of existence of domains 18

2.2.3. The dynamic behavior of domains 19

2.2.4. Bulk behavior magnetization 20

2.2.5. The Magnetization Curve 21

2.2.6. Units for the Magnetization Curve 22

2.2.7. Conversion between Bohr Magnetons and Magnetization 23

2.2.8. Flux Lines 23

2.2.9. Hysteresis behavior 24

2.2.10. Minor Loops 25

2.3 Historical Background of Permeability in Ferrites 26

1. Effect of Iron Content on Permeability 27
2. Ferric Ion Substitution 28
3. Effect of divalent ion variation 29
4. Permeability dependence on Zinc 29
5. Effect of cobalt on permeability 30
6. Oxygen Stoichiometry 30
7. Effect of Foreign Ions on Permeability 31

2.4 Recent Trends in Permeability of MnZn Ferrites 32

2.5 Microstructural aspects of Permeability of Ferrites 40

1. Effect of grain size on permeability 40
2. Exaggerated grain growth in ferrites 41
3. Duplex grain structure 42
4. Effect of porosity on permeability 43

CHAPTER-3 EXPERIMENTAL WORK 45

3.1 Ferrite-Processing 46

3.1.1 Powder Preparation 46

1. Dry Mixing 46
2. Calcination 46
3. Milling 47
4. Drying and Granulation 48
5. Forming 48

3.1.2 Sintering 49

3.2 Characterization 51

CHAPTER –4 RESULTS AND DISCUSSION 53

4.1 Inductance value and initial magnetic permeability 54

4.2 Variation of Permeability with frequency 55

4.3 Variation in permeability with temperature 57

4.4 Comparison of Curie temperature 60

4.5 Microstructure Investigation 61

CHAPTER -5 CONCLUSION AND SCOPE FOR FUTURE WORK 64

5.1 Conclusion 65

5.2 Scope of Future work 65

REFERENCES…… 66

CHAPTER 1

Introduction

CHAPTER 1

INTRODUCTION

In the recent times, Iron and its alloys were used as magnetic materials for the applications in the electrical industry. However, with the discovery of higher frequencies, the customary techniques to reducing eddy current losses, using lamination or iron powder cores, were no longer efficient or cost effective. This realization stimulated a renewed interest in "magnetic insulators" as first reported by S. Hilpert in Germany in 1909. It was readily understood that if the high electrical resistivity of oxides could be combined with desired magnetic characteristics, a magnetic material would result that was particularly well suited for high frequency operation.

Research in order to develop this type of material, was undertaken in various laboratories all over the world, such as by V. Kato, T. Takei, and N. Kawai in the 1930's in Japan and by J. Snoek of the Philips Research Laboratories in the period 1935-45 in the Netherlands. By 1945 Snoek had laid down the basic fundamentals of the physics and technology of practical ferrite materials. In 1948, the Neel theory of ferromagnetic provided the theoretical understanding of this type of magnetic material.

These ferrites are ceramic, homogeneous materials composed of various oxides with iron oxide as their main constituent. Based upon the chemical composition, soft ferrites can be divided into two major categories, manganese-zinc ferrite and nickel-zinc ferrite. In each of these categories many different Mn-Zn and Ni-Zn material grades are being manufactured by varying the chemical composition or by different manufacturing techniques. The two families of Mn-Zn and Ni-Zn ferrite materials complement each other and allow the use of soft ferrites from audio frequencies to several hundred mega-hertz. The first practical soft ferrite application was in inductors used in LC filters in frequency division multiplex equipment. The combination of high resistivity and good magnetic properties made these ferrites an excellent core material for these filters operating over the 50-450 kHz frequency range. The large scale introduction of TV in the 1950's was a major opportunity for the fledgling ferrite industry. In TV sets, ferrite cores were the material of choice for the high voltage transformer and the picture tube deflection system. For four decades ferrite components have been used in an ever

widening range of applications and in steadily increasing quantities, a few are mentioned in table-1 below.

Table 1 - Soft ferrite applications.

SOFT FERRITE APPLICATIONS	
MAGNETIC DEVICES	**APPLICATION**
Power transformers and Chokes	High frequency power supplies
Inductors and tuned transformers	Frequency selective circuits
Pulse and wide band transformers	Matching devices
Magnetic deflection structures	TV sets and monitors
Recording heads	Memory storage devices
Rotating transformers	VCR's
Transducers	Vending machines and ultrasonic cleaners

Table 2 - Merits and demerits of ferrites over other magnetic materials.

FERRITES VERSUS OTHER MATERIALS	
ADVANTAGES	**DISADVANTAGES**
High resistivity	Low saturation flux density
Wide range of operating frequencies	Poor thermal conductivity
Low loss combined with high permeability	Low tensile strength
Time and temperature stability	Brittle material
Large material selection	
Versatility of core shapes	
Low cost	

These cubic ferrites are especially useful due to two key characteristics :

- High magnetic permeability, which concentrates and enhances the magnetic field.
- High electrical resistivity, which ensures total penetration of the electromagnetic (EM) field.

Furthermore, the dominance of ferrites rests upon a remarkable flexibility in providing tailor-made solutions, ease of preparation, and price and performance considerations. Hence ferrites are widely manufactured into circuit elements, like inductors and cores, reading-writing heads and information storage media.

Amongst the soft ferrites, Manganese Zinc Ferrites are most common, and are used in many more applications than their counterparts, such as nickel-zinc ferrites. Within the Mn-Zn category, large varieties of materials are possible, and the material selection is mainly a function of the application that needs to be accommodated. The application dictates the desirable material characteristics, which in turn determines the chemical composition of the ferrite material. Manganese zinc ferrites are primarily used for frequencies less than 2 MHz. Figure-1 shows the composition diagram for MnZn ferrites in mole% for Ferric oxide, Manganese oxide and Zinc oxide. It identifies the composition which gives optimum performance for saturation flux density (B_s), low losses (Q) and high initial permeability (μ_i). It also identifies the Curie temperature (T_C) lines for 100 and 250°C. From this composition chart, it is clear that not one composition, of Mn ferrite, can fulfill all design objectives.

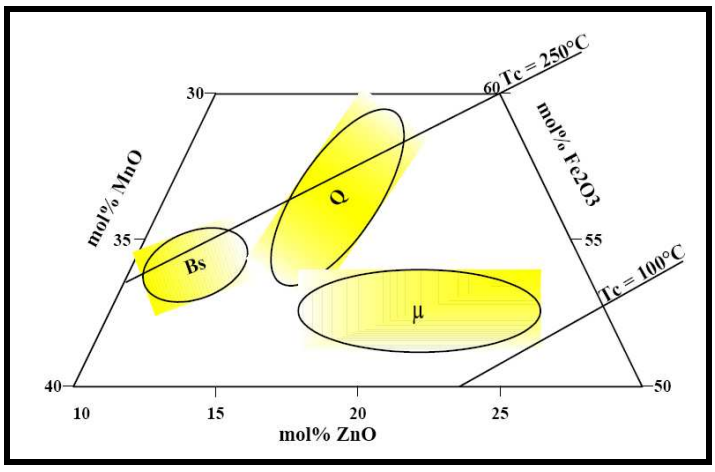

Figure 1 - Composition Diagram for Mn-Zn ferrites.

Nickel Zinc ferrites are characterized by their high material resistivity, several orders of magnitude higher than MnZn ferrites. Because of its high resistivity NiZn ferrite is the material of choice for operating from l-2 MHz to several hundred MHz. To cover such a wide frequency range and different applications, a large number of nickel-zinc materials have been developed over the years. Use of Nickel Zinc ferrites is limited due to their increasing cost. It should be noted that certain nickel chemistries are stress sensitive and can be adversely changed by some types of stress; this may be a mechanical shock or any grinding operations. Strong magnetic fields from holding devices and fixtures or magnetic chucks used in machining operations may also provide this stress. These resulting changes can include variation in permeability and core loss (lowering of Q). These changes cannot be reversed by degaussing or other electric/magnetic processes.

Manganese Zinc ferrite has the highest permeability and saturation induction of the ferrite class of materials and has the advantage of various stoichiometries with nearly zero magneto-crystalline anisotropy and magneto-restriction, important for stress insensitivity and low noise.

CHAPTER

2

Literature Survey

CHAPTER- 2

FERRITES : AN OVERVIEW

2.1 Crystal Structures of Ferrites

Ceramic magnets have become firmly established as electric and electronic engineering material; most contains iron as a major constituent and are collectively called ferrites. From the point of view of electric properties these are semi-conductors or insulators, in contrast to metallic magnetic materials which are electric conductors**.** Consequence of this is that the eddy currents produced by the alternating magnetic fields which many devices generate are limited in ferrites by their high intrinsic resistivities.

Magnetic structures of increasing complexity starts from the spinning and orbital motion of electron, progressing to atom, and finally focuses on domain. Although domain is important in explaining cooperative magnetic phenomena, the next larger physical magnetic entity after the ion is ferrite unit cell or crystal structure.

The crystal structure of ferrites can be regarded as an interlocking networking of positively charged metal ions (Fe^{3+} , M^{2+}) and negatively charged divalent oxygen ions (O^{2-}).The arrangement of the ions or the crystal structure of the ferrite plays an important role in determining the magnetic interactions.

CLASSES OF CRYSTAL STRUCTURES IN FERRITES

In ferrites, various crystal structures preferred is determined with size and charge of the metal ions that balance the charge of oxygen ions and the relative amounts of these ions. There are three crystal structures mostly available in case of ferrites. These are:

1. Spinal Structure
2. Garnet structure
3. Hexa-ferrite structure.

1. <u>Spinal structure</u>:-

The spinal is by far the most widely used ferrites. The spinal structure is derived from the mineral spinal ($MgAl_2O_4$ or $MgO.Al_2O_3$) whose structure was elucidated by Bragg. Analogous to the mineral spinal the magnetic spinal have general formula $MO.Fe_2O_3$, where M is divalent metal ion. The trivalent aluminum is usually replaced by Fe^{+++} or Fe^{+++} in combination with any other trivalent ion . Although the great majority of ferrites contain iron oxide as name implies, but there are some "ferrites" based on Cr, Mn , and other elements. Although Mn, Cr are not ferromagnetic elements, in combination with other elements such as oxygen and other metal ions, they can behave as magnetic ions.

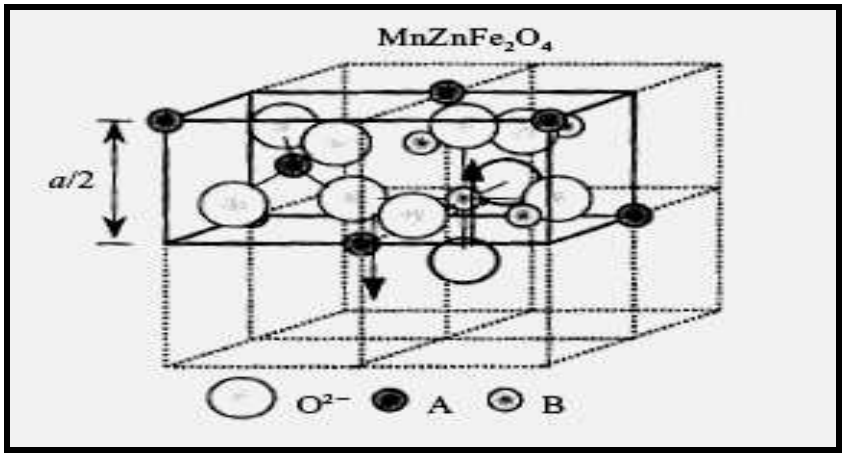

Figure-3 structure of Mn-Zn Ferrite

Ion Charge Balance and Crystal structure:-

The spinal lattice is composed of a close packed oxygen arrangement in which 32 oxygen ions form a unit cell which is the smallest repeating unit in crystal network . Between the layers of oxygen ions, there are the interstices that may accommodate the metal ions. Not all the interstices are same; some which would be called **A** sites are surrounded with four nearest neighboring oxygen ions and are called tetrahedral sites. The other type of sites (**B** sites) is coordinated by six neighboring oxygen ions whose centre connecting lines describe an octahedron . The **B** sites are called octahedral sites . In the unit cell of 32 oxygen ions there are 64 tetrahedral sites and 32 octahedral sites . If all the sites are filled with metal ions , of ether +2 or +3 valence, the positive charge

would be much greater than the negative charge and so the structure will be much greater than negative charge. Due to which the structure will be electrically neutral . It turns out that of the 64 tetrahedral sites , only 8 are occupied and out of the 32 octahedral sites, only 8 are occupied . If , as in the mineral spinal the tetrahedral are occupied by divalent ions and the octahedral sites are occupied by the trivalent ions, the total positive charge will be $8\times(+2) = +16$ plus the $16 \times (+3) = +48$, or a total of +64 which is needed to balance the $32\times(-2) = -64$ for the oxygen ions. Then there would be eight formula units of $MO.Fe_2O_4$.

Site Preference of the Ions:

The preference of the individual ions for two type of lattice sites is determined by:

1. The ionic radii of the specific ions
2. The size of interstices
3. Temperature
4. The orbital preference for specific coordination

Table 3 : Metal ions involved in Spinal ferrites

METAL ION	***IONIC RADIUS*** **(Angstronm Units, A^0)**
Mg^{++}	0.78
Mn^{++}	0.91
Mn^{+++}	0.70
Fe^{++}	0.83
Fe^{+++}	0.67
Co^{++}	0.82
Ni^{++}	0.78
Cu^{++}	0.70
Zn^{++}	0.82
Cd^{++}	1.03
Al^{+++}	0.57
Cr^{+++}	0.64

The divalent ions are generally larger than the trivalent , octahedral sites are also larger than tetrahedral , Therefore it would be reasonable that trivalent ions go into tetrahedral sites and divalent goes to the octahedral sites.

Two exceptions are found in Zn^{++} and Cd^{++} which prefer tetrahedral sites because electronic configuration is favorable for tetrahedral bonding to oxygen ions.

Normal Spinals:

In a unit cell of spinal lattice, eight tetrahedral and sixteen octahedral sites are occupied by metal ions. In case of mineral spinals the divalent ion (Mg) occupy the **A** site and trivalent ion (Al) the **B** sites , this is known as *normal spinal*.

Inverse Spinals:

Barth and Posnak (1915) found many cases in which the trivalent ions preferred the **A** sites and filled these first . Spinals showing this type of structure are known as *inverse spinals.*

2. <u>Hexagonal Ferrites</u>:

This class of magnetic oxide is called megnetoplumbite structure from the mineral of the same name. Whereas the symmetry of the spinal crystal structure is cubic, that for the megnetoplumbite structure is hexagonal. Thus, it has a major preferred axis called **C** axis. The preferred direction is used to good advantage for permanent magnetic material.

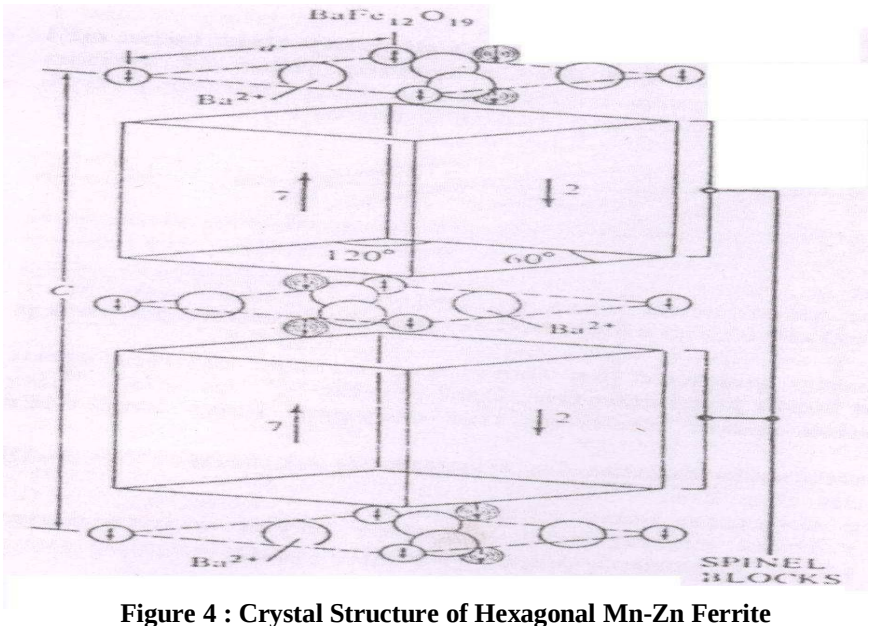

Figure 4 : Crystal Structure of Hexagonal Mn-Zn Ferrite

The megnetoplumbite unit cell contains a total of ten layers, two of which contain M^{++} ion: four layers of oxygen ions each: followed by a layer of three oxygen ions and one M^{++} ion; again followed by four oxygen layers of four ions each: and another layer containing the three oxygen ions and one M^{++} ion but situated diametrically opposite to the M^{++} ion in the previous layer containing M^{++}.

The Fe^{+++} ions are located in the interstices of these ten layers. There are octahedral and tetrahedral sites, as well as one more type not found in the spinal structure in which the metal ion is surrounded by five oxygen ions forming a trigonal bi pyramidal in the same layer of the M^{++} ion.

The megnetoplumbite formula is $MFe_{12}O_{19}$, where M can be Ba, Sr, or Pb. There are two formula units per unit cell. Per formula unit, the moments of the 12 Fe^{+++} ions are arranged with the spins of 12 in the up direction and 8 in the down direction, giving a predicted net moment of 4 Fe^{+++} ions per formula unit time 5 per ion, or a total of 20 per formula unit.

3. <u>Magnetic rare earth garnets:</u>

Magnetic garnets crystallize in the dodecahedral or 12-sided structure related to the mineral garnet. The general formula is $3M_2O_3 5Fe_2O_3$ or $M_3Fe_5O_{12}$. Note that in this case all the metal ions are trivalent in contrast to the other two classes. In the important magnetic garnet, M is usually yttrium (Y) or one of the rare earth ions. Even though

yttrium is not a rare earth ion, it behaves as one and therefore is included in the designation rare earth garnets. The ions La^{+++}, Ca^{+++}, Pr^{+++}, and Nd^{+++} are too large to form simple garnets but may form solid solutions with other rare earth garnets.

Magnetic garnets were discovered by Bertaut and Forrat (1956) and independent by Geller and Gaileo (1957) at about the same time. The crystal structure of magnetic garnets was elucidated by Geller and Gilleo (1957). There are three different types of sites for garnets (a) tetrahedral (b) octahedral; and (c) dodecahedral sites. The unsubstituted garnets that have only trivalent ions are very stoichiometric, so that they involve fewer preparation problems compared to the spinels.

The rare earth ions are large, and so they occupy the large dodecahedral sites. There are 16 octahedral, 24 tetrahedral, and 24 dodecahedral sites in a unit cell containing eight formula units. One formula unit, $3M_2O_3 5Fe_2O_3$, is distributed as follows:

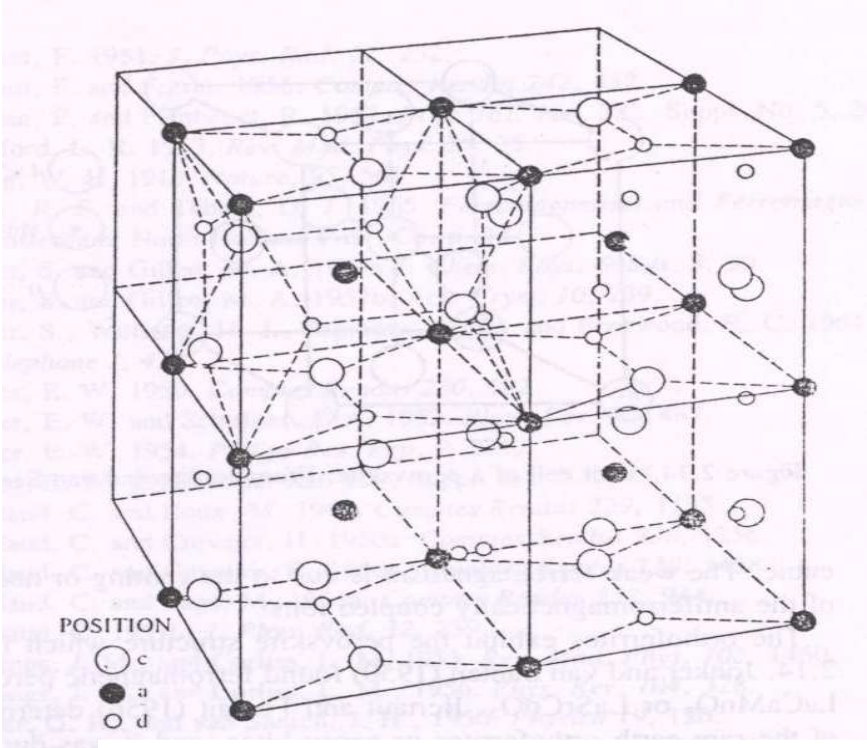

Figure 5: Crystal structure of Magnetic rare earth garnet

$3M_2O_3$ –dodecahedral (c)

$3Fe_2O_3$ –tetrahedral (a)

$2Fe_2O_3$-octahedral (d)

The moments of the Fe^{+++} ions on the octahedral sites are antiferromagnetically coupled to the moments of the Fe^{+++} ions on the tetrahedral sites. Similarly, moments of the M^{+++} ions on the dodecahedral sites are also coupled to the tetrahedral sites and, as previously mentioned, may contribute to the magnetization of that sublattice. In the absence of the rare earth ion contribution as in the most important of the series, $3Y_2O_3.Fe_2O_3$, all the moments are due to the Fe^{+++} ions. Formula this formula unit, the net resultant moment is due to the $2Fe^{+++}$ on the tetrahedral.This gives 2 x 5 for Fe^{+++} = 10

2.2 THE MAGNETIZATION IN DOMAINS AND BULK MATERIALS

1. The nature of domains:

In a ferromagnetic domain, there is parallel alignment of the atomic moments. In a ferrite domain, the net moments of the antiferrimagnetic interactions are spontaneously oriented parallel to each other (even without an applied magnetic field). The term, spontaneous magnetization or polarization is often used to describe this property. Each domain becomes a magnet composed of smaller magnets (ferromagnetic moments). Domains contain about 10^{12} to 10^{15} atoms and their dimensions are on the order of microns (10^{-4} cm.). Their size and geometry are governed by certain considerations. Domains are formed basically to reduce the magnetostatic energy which is the magnetic potential energy contained in the field lines (or flux lines as they are commonly called) connecting north and south poles outside of the material. Figure 6 shows the lines of flux in a

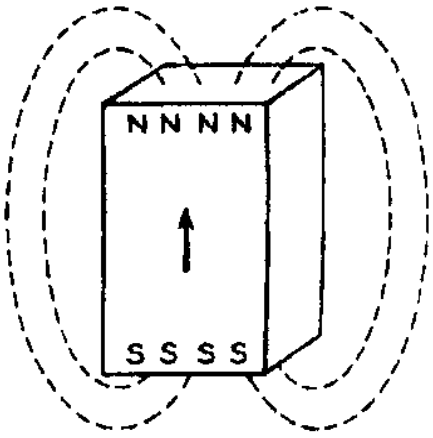

Figure 6 Lines of force in a particle of a single domain

Particle with a single domain. The arrows indicate the direction of the magnetization and consequently the direction of spin alignment in the domain. We can substantially reduce the length of the flux path through the unfavorable air space by spitting that domain into two or more smaller domains. This is shown in Figure 7. This splitting process continues to lower the energy of the system until the point that more energy is required to form the domain boundary than is decreased by the magnetostatic energy change. When a large domain is split into *n* domains, the energy of the new structure is about *l/n th* of the single domain structure. In Figure 7, the moments in adjacent domains

Called closure domains. In this configuration, the magnetic flux path never leaves the

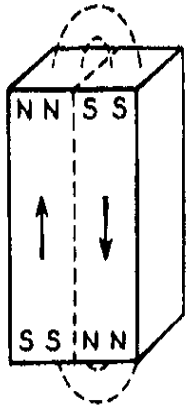

Figure 7- Reduction of magnetostatic energy by the formation of domains

boundary of the material. Therefore, the magnetostatic energy is reduced. This type of structure may also be found at the outer surfaces of a material. The size and shape of a domain may be determined by the minimization of several types of energies.They are;

a. Magnetostatic energy
b. Magnetocrystalline anisotropy energy
c. Magnetostrictive energy
d. Domain wall energy

In addition, certain microstructural imperfections such as voids, non-magnetic in-clusions and grain boundaries may also affect the local variations in domain structure.

a. Magnetostatic Energy

The magnetostatic energy is the work needed to put magnetic poles in special geometric configurations. It is also the energy of demagnetization. It can be calculated for simple geometric shapes. For an infinite sheet magnetized at right angles to the surface the equation (Bozorth 1951) for the magnetostatic energy per cm^3 is ;

$$E_p = 2\pi M_s^2$$

Neel (1944) and Kittel (1946) have calculated the magnetostatic energy of flat strips of thickness, d, magnetized to intensity, M, alternately across the thickness of the planes. The equation is;

$$E_p = 0.85\ dM^2$$

The calculations for other shapes come out with the general formula;

$$E_p = (\text{Constant})\ x\ dM_s^2$$

Therefore the magnetostatic energy is decreased as the width of the domain de-creases.This mathematically confirms our assumption that the splitting of domains into smaller widths decreases the energy from the magnetostatic view. In fact, the energy of the domain structure is one thousandth that of a similar sized single do-main.

b. Magnetocrystalline Anisotropy Energy

Most matter is crystalline in nature; that is, it is composed of repeating units of definite symmetry. When we take a common geometrical configuration that may form the smallest repeating unit, namely a cube. Atoms or molecules are usually located at corners of the cube and in addition, at either the center of the cube or at the centers of the 6 faces. In most magnetic materials, to varying degree, the domain magnetization tends to align itself along one of the main crystal directions. This direction is called the easy direction of magnetization. Sometimes it is an edge of the cube and at other times, it may be a body diagonal. The difference in energy of a state where the magnetization is aligned along an easy direction and one where it is aligned along a hard direction is called the magnetocrystalline anisotropy energy. This magnetocrystalline anisotropy energy is also that needed to rotate the moment from the easy direction to another direction The energy of the domain can be lowered by this amount by having the spins (ferromagnetics) or

moments (ferrimagnetics) align themselves along these directions of easy magnetization. In materials with high uniaxial anisotropy energy the moment of one domain is usually aligned along an easy direction of magnetization. Then, the adjacent domain will have the same tendency to align along the same axis but in the opposite direction. Even in materials with lower anisotropy, the 180° wall is often found. In crystals of cubic symmetry, where many of the major axes are at right angles(such as the cube edges) the 90° domain wall is also a reasonable possibility.

Magnetocrystalline anisotropy is due to the fact that there is not complete quenching of the orbital angular momentum as we postulated originally. With a small orbital moment that is mechanically tied to the lattice, the spin system can couple to it and therefore indirectly affect the lattice or the dimensions of the material.

c. <u>Magnetostrictive Energy:</u>

When a magnetic material is magnetized, a small change in the dimensions occurs.The relative change is on the order of several parts per million and is called magnetostriction. The converse is also true. That is, when a magnetic material is stressed, the direction of magnetization will be aligned parallel to the direction of stress in some materials and at right angles to it in others. The energy of magnetostriction depends on the amount of stress and on a constant characteristic of the material called the magnetostriction constant.

$$E = 3/2\ \lambda\sigma$$

where; λ = magnetostriction constant

σ = Applied stress

The convention of the sign of the magnetostriction constant is such that if the magnetostriction is positive, the magnetization is increased by tension and also the material expands when the magnetization is increased. On the other hand, if the magnetostriction is negative, the magnetization is decreased by tension and the material contracts when it is magnetized. Magnetostriction as in the case of anisotropy is due to incomplete orbital quenching and the so-called spin-orbit, L-S or Russell Saunders coupling. Stresses can be introduced in ferrites by mechanical and thermal operations such as firing, grinding, and

tumbling. These stresses also affect the directions of the moments locally depending on the distribution of the stresses.

d. <u>Domain Wall Energy:</u>

Although Weiss (1907) first came up with the idea of the strong molecular field producing regions of oriented atomic moments or of spontaneous magnetization, it was Bloch(1932) who was the first to present the idea of magnetic domains, with domain walls (sometimes called Bloch walls) or boundaries separating them. In the domain structure of bulk materials, the domain wall or boundary is that region where the magnetization direction in one domain is gradually changed to the direction of the neighboring domain. If 5 is the thickness of the domain wall which is proportional to the number of atomic layers through which the magnetization is to change from the initial direction to the final direction, the exchange energy stored in the transition layer due to the spin interaction is;

$$E_e = kT_c/a$$

where kT_c= Thermal energy at the Curie point

a= Distance between atoms

Therefore the exchange energy is reduced by an increase in the width of the wall or with the number of atomic layers in that wall. However, in the presence of an anisotropy energy or preferred direction, rotation of the magnetization from an easy direction increases the energy so the wall energy due to the anisotropy is:

$$E_k = k\,\delta$$

In this case, the energy is increased as the domain width or number of atomic layers is increased. The two effects oppose each other and the minimum energy of the wall per unit area of wall occurs according to the following equation;

$$E_w = 2(K_a T_c/a)^{1/2}$$

where K_a= Anisotropy constant (described later)

If magnetostriction is a consideration, the equation is modified to;

$$E_w = 2(kT/a)^{1/2}\,(K_a + 3\,\lambda_s\,\sigma/2)^{1/2}$$

where λ_s = magnetostriction constant

Typical values of domain wall energies are on the order of $1\text{-}2\ \text{ergs/cm}^2$ The domain wall thickness for the condition of minimum energy is given by the equation;

$$\delta = (\text{Constant})\ x\ a(E/K)^{1/2}$$

Typical calculated values of δ are about 10^3 A^0 or about 10^{-5} cm. With some soft magnetic materials the value may be about 10^{-6} cm while in some hard materials, the value may be on the order of $l0^{-4}$ cm. or about one micron. The whole array of domains will be arranged in such a way as to minimize the total energy of the system composed mainly of the above four energies.

2. Proof of existence of domains:

The earliest experimental indication that domains existed was presented by Barkhausen (1919) who was able to pick up small voltages due to the discontinuous changes in the magnetizations in these regions . Barkhausen amplified these voltages many times

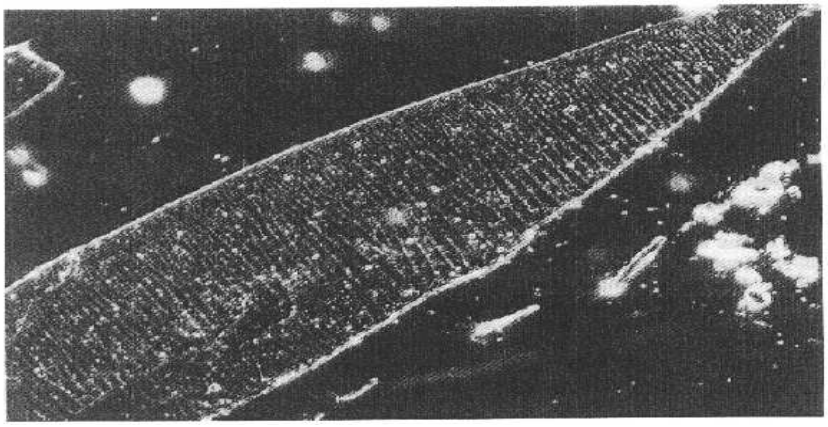

figure .8 (a) Visualization of magnetic domains by means of the Bitter magnetic particle technique. The white stripes are the domain walls.

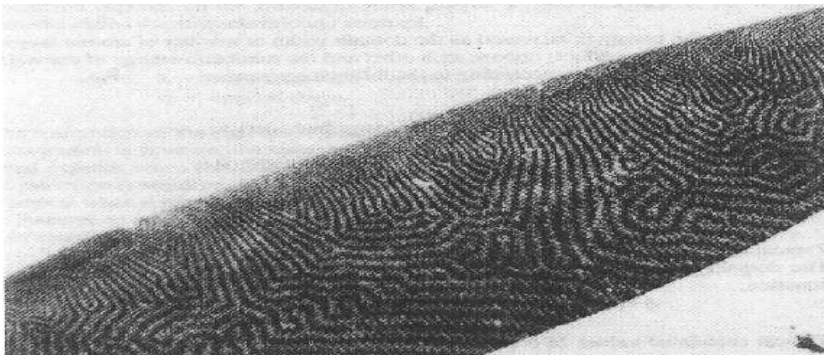

figure 8 (b) Visualization of domains by Faraday rotation with polarized light

and made them audible on a loudspeaker. Bitter (1931) was first able to visualize domains by spreading over the sample, a suspension of colloidal magnetite.The colloidal particles will be concentrated at the domain boundaries since large field gradients exist there. These arrangements are called Bitter patterns. Figure 8a exhibits domain walls using this method. This technique is limited to the static state since the powder prohibits true dynamic observations as well as temperature restrictions. Since light is an electromagnetic wave, it might be expected to interact with magnetic fields and moments. Many so-called magneto-optic effects have been observed. Through this interaction, domains have been made visible microscopically by both reflected and transmitted light. One technique employs a polarized light which has its plane of polarization rotated differently by domains with different magnetization direction. When the rotated light beam is sent through a polarizing medium called the analyzer, the domains will show up because of the contrast in light intensities of the neighboring domains. With reflected light, this phenomenon is known as the Kerr effect. With transmitted light, it is called Faraday rotation. Domain patterns in many magnetic materials have been photographed using this technique. Figure 8b is an example of the Faraday technique. Kaczmarek(1992) used the transverse and longitudinal Kerr Effects to observe do-mains in soft polycrystalline ferrites. Using a laser and fiber optics, he examined hysteresis effects that are in good relationship with bulk measurements

Domain patterns have also been viewed by TEM (Transmission Electron Microscopy). Vander Zaag (1992) studied domain structures in MnZn ferrites using this technique. He found that at a grain size up to 4 microns, the grains were mono-domain while above this size, they were polydomain.

3. The dynamic behavior of domains:

Two general mechanisms are involved in changing the magnetization in a domain and, therefore, changing the magnetization in a sample. The first mechanism acts by rotating the magnetization towards the direction of the field. Since this may involve rotating the magnetization from an axis of easy magnetization in a crystal to one of more difficult magnetization, a certain amount of anisotropy energy is required. The rotations can be small as indicated in Figure 9 or they can be almost the equivalent of a complete 180°

reversal or flip if the crystal structure is uniaxial and if the magnetizing field is opposite to the original magnetization direction of the domain. The other mechanism for changing the domain magnetization is one in which the direction of magnetization remains the same, but the volumes occupied by the different domains may change. In this process, the domains whose magnetizations are in a direction closest to the field direction grow larger

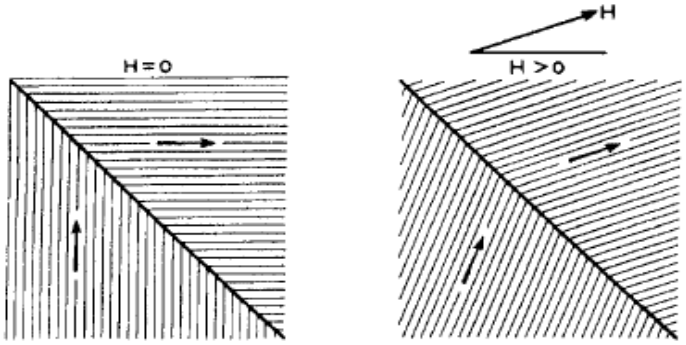

figure 9 Change of domain magnetization by domain wall movement

while those that are more unfavorably oriented shrink in size. This process which is called domain wall motion. The mechanism for domain wall motion starts in the domain wall. Present in the wall is a force (greatest with the moments in the walls that are at an angle of 90° to the applied field) that will tend to rotate those moments in line with the field. As a result, the center of the domain wall will move towards the domain opposed to the field. Thus, the area of the domain with favorable orientation will grow at the expense of its neighbor.

4. <u>Bulk behaviour magnetization:</u>

We have proceeded through the hierarchy of magnetic structures from the electron through the domain. Although domains are not physical entities such as atoms or crystal lattices and can only be visualized by special means, for the purpose of magnetic structure they are important in explaining the process of magnetization. We now can discuss why a material that has strongly oriented moments in a domain often has no resultant bulk material magnetization. We can also examine why this apparently "non-magnetic" material can be transformed into a strongly magnetic body by domain dynamics discussed above. The answer, of course, resides in the fact that, if the material

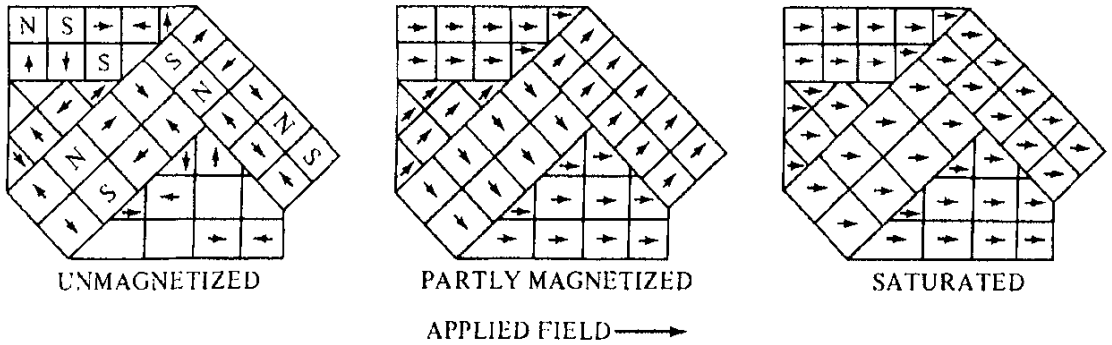

figure10 Stages in Magnetization of a sample containing several crystals

has been demagnetized, the domains point in all random directions so that there is complete cancellation and the resultant magnetization is zero (Figure 5). The possible steps to complete orientation of the domains or magnetization of the material are also shown in Figure 10.

5. The Magnetization Curve*:*

We are now ready to look at the bulk magnetic properties of a material. Thus far, the magnetic moment or the magnetization has been given in either atomic units (or Bohr magnetons) or in physical units based on action of magnets. How can we re-late these to actual material properties? The Bohr magnetons were based on limiting values at absolute zero and since it was an atomic moment (ferromagnetism) or a resultant or combination of moments (ferrimagnetism), it was in the so called saturated condition. Having said that, there is a zero net moment in unmagnetized bulk materials, we can predict that there will be an infinite number of degrees of magnetization between the unmagnetized and saturation conditions. These extreme situations correspond, respectively, to random orientation of domain to complete alignment in one direction with the elimination of domain walls. If we start with a demagnetized specimen and increase the magnetic field, the bulk material will be progressively magnetized by the domain dynamics described previously.

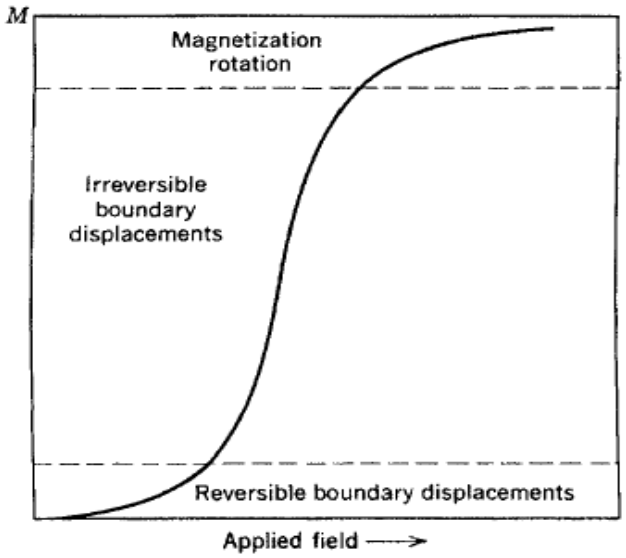

Figure 11 Domain dynamics during various parts of the magnetization curve

The magnetization of the sample will follow the course shown in Figure 11. The slope from the origin to a point on the curve or the ratio M/H has previously been defined as the magnetic susceptibility. This curve is called the magnetization curve. The curve is generally perceived as being made up of three major divisions.

The lower section is called the initial susceptibility region in which there are reversible domain wall movements and rotations. Being reversible means that, after changing the magnetization slightly with an increase in field, the original magnetization condition can be returned if the field is reduced to the original value. The second stage of the magnetization curve in which the slope increases greatly is one in which irreversible domain wall motion occurs. The third section of the curve is one of irreversible domain rotations. Here, the slope is very flat indicating the large amount of energy that is required to rotate the remaining domain magnetization in line with the magnetic field.

6. Units for the Magnetization Curve:

We have described the unit of magnetizing field H, from the interaction of magnetic poles. The unit was the oersted, defined as the field experienced at a distance of 1cm from a unit pole. We have also described the magnetic moment, ml, from the dipole. The pole density in poles per unit cross sectional area is the intensity of magnetization, M, whose units are the same as moment/unit volume = emu/cm^3.

7. Conversion between Bohr Magnetons and Magnetization:

There are times when we have to convert the moment in Bohr magnetons per atom, ion or formula unit in the case of ferrites to units of bulk magnetization, M, in emu/cm^3 or in units of emu/g. The former, M, is more important in magnetic design as part of the magnetic flux. The latter, a, is important for materials research since with temperature changes, the density must be known accurately at each temperature.

The pertinent formula is:

$$M = n \times \mu_B \times N_o \times d/A$$

Where; N_o= Number of atom/mole (6.02×10^{23})

A= Atomic weight

n= number of unpaired electron spins/atom

μ_B = value of a Bohr magneton

d = Density

The value $n \times \mu_B$ is the moment of the atom or ion in emu.

8. Flux Lines:

Faraday found it convenient to liken magnetic behavior to a flow of endless lines of induction that indicated the direction and intensity of he flow. He called these lines flux lines and the number of lines per unit area the flux density or magnetic induction, B. The flux is composed of H lines and M lines. A schematic representation of the flux is given in Figure 12. Note that the lines traverse the sample, leave it at the North pole, and return at the South pole. In cgs units, the induction or flux density, B, is given by;

$$B = H + 4\pi M$$

A unit pole gives rise to a unit field everywhere on the surface of a sphere of unit radius.

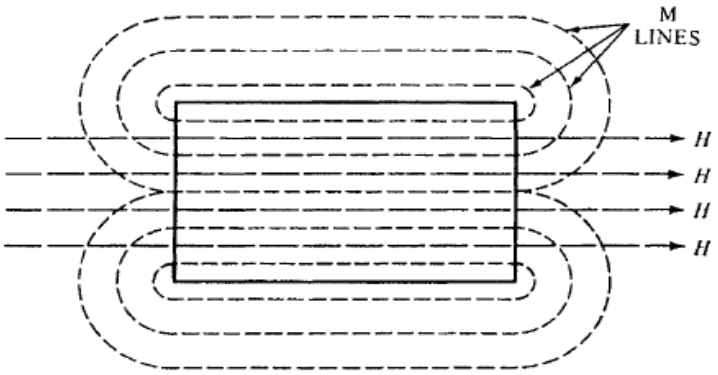

Figure 12 Magnetic flux lines composed of H (field) and M

The area of this sphere is 4TC cm^. The cgs unit of induction is the gauss. The units for the lines of induction or flux are known as Maxwell or just plain "lines". Therefore, the units for flux density, B, are maxwells/cm^3. B can also be Figure 8-Magnetic flux lines composed of H (field) and M (magnetization lines defined by the voltage generated in a wire wound around a core of magnetic material in which there are known variations of flux with time.

9. <u>Hysteresis behavior:</u>

In magnetic applications, we are interested in how much induction a certain applied field creates. In soft magnetic materials, we want a high induction for a low field. In this case, H is very small compared to 4 π M and B is essentially equal to 4πM. In the case of a permanent magnet, the H component can amount to from 50% or more of the total B. If we start with a demagnetized specimen and increase the magnetic field, the induction increases as shown in Figure 13. At high fields, the induction flattens out at a value called the saturation induction, Bg. If, after the material is saturated, the field is reduced to zero and then reversed in the opposite direction, the original magnetization curve is not reproduced but a loop commonly called a hysteresis loop is obtained. Figure 13 shows such a hysteresis loop with the Initial magnetization curve and hysteresis loop magnetization curve included. The arrows show the direction of travel. We notice that there is a lag in the induction with respect to the field. This lag is called hysteresis. As a result, the induction at a given field strength has 2 values and cannot be specified without a knowledge of the previous magnetic history of the sample. The area

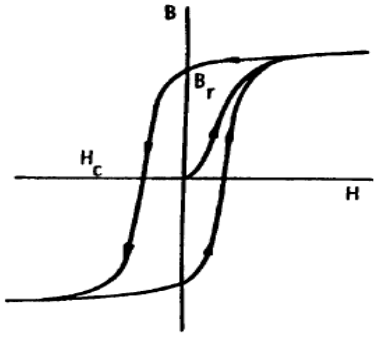

Figure 13

Initial magnetization curve and hysteresis loop

included in the hysteresis loop is a measure of the magnetic losses incurred in the cyclic magnetization process. The hysteresis losses can also be correlated with the irreversible domain dynamics we had previously mentioned. The value of the induction after saturation when the field is reduced to zero is called the remanent induction or remanence or retentivity, (B_r). The values of the reverse field needed after saturation to reduce the induction to zero is called the coercive force or coercivity, (H_c). The unit for H_C is the oersted and that for B_r is the gauss. Both of these properties are very important and we shall refer to them in almost every magnetic application.

10. Minor Loops:

The condition of the magnetization process when the material is magnetized to saturation, is not always true and loops can be produced when varying degrees of magnetization are produced. When the maximum induction is less than saturation, the loop is called a minor loop. The shape of these minor loops can be vastly different than the saturated loop.

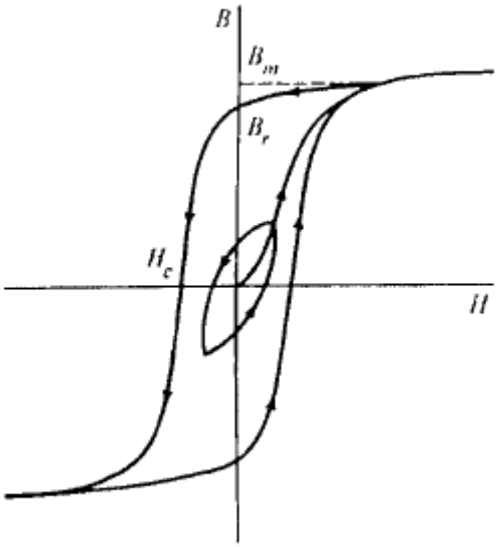

figure 14 A minor hysteresis loop with the saturation loop

When an unmagnetized sample is progressively magnetized it follows the magnetization curve. If we stop part of the way up and then reduce the field to zero and repeat the process to the same value of reverse field the result is a minor loop. A minor loop is shown in Fig 14 along with the saturation loop.

2.3 HISTORICAL BACKGROUND OF PERMEABILITY IN FERRITES

The magnetic permeability may be considered to be a measure of the efficiency of a magnetic material. That is, it tells us how much polarization of magnetization our input of magnetizing force will give us. In metallic magnetic materials that have much higher saturation magnetizations than ferrites, the highest permeabilities are not usually present in the materials with the highest saturations. The reason why is the dominance of other intrinsic factors such as low magnetostrictions and anisotropies, coupled with good extrinsic factors such as very clean grain boundaries and low residual stresses after annealing. In ferrites, on the other hand, the saturations are lower, the microstructure is not as clean (thicker grain boundaries), and many firing stresses remain. For reversible rotational processes, Chikazumi [1] gave the permeability (1964) as

$$(\mu - 1) = (\text{constant}) M_s^2 \sin^2 \text{Ø} / K_1$$

where Ø = angle between M and H

For reversible wall processes, the permeability is

$$(\mu - 1) = (\text{constant}) M_s^2 S$$

where, S = wall surface area

= Second derivative of the wall energy with respect to wall displacement

We can see that both the permeability caused by domain rotation and that caused by domain wall movement are related to $M_s^{2.}$ It is not surprising to find the higher permeabilities in ferrites in the higher saturation Mn-Zn ferrites compared to the others. Of course, the low anisotropy and magnetostriction also help. In fact, high saturation is certainly not the only requirement for high permeability inasmuch as magnetite has a high saturation but very low permeability even at low AC frequencies because of the high eddy current losses.

Manganese zinc ferrites have higher permeabilities at low or medium frequencies. When the frequencies involved are in the upper megahertz range, the permeability drops off owing to the great increase in losses.

1. Effect of Iron Content on Permeability

The metal ion present in the largest concentration mole wise in ferrites is Fe^{3+}, and since it has a high ionic moment (5 μ_B) it has the highest potential for controlling the magnetic characteristics. In the completely inverse ferrites such as $NiFe_2O_4$, the large moments of the two Fe^{3+} sublattices cancel each other, and no advantage is taken of the potential Fe^{3+} moment. The large moment of Fe^{3+} is used in the zinc-substituted mixed ferrites in which the Fe^{3+} ions on the two sublattices are disproportionated. These effects are not chemical. With the great variety of possible chemistries of spinal ferrites, the Fe_2O_3 content of the finished ferrite is the least varied of all the metal ions since it is pegged at 50 mole percent by the spinal formula ($MO.Fe_2O_3$). In most commercially important Mn-Zn ferrite materials, the starting mix may contain slightly more than 50 mole percent of Fe_2O_3. The purpose of the extra ion is to improve the magnetic properties by the formation of Fe^{2+} ions. One such basic property is the magnetostriction which is defined as change in the length of a material when it is subjected to a magnetic field.

The magnetostrictions of several ferrites are shown in the table. Note that ferrous ferrite is the only ferrite that has positive magnetostriction. Therefore, it would be useful to minimize the net magnetostriction by compensating the negative values of the other ferrites through the incorporation of ferrous ferrite as a part of the solid solution. Ferrous ferrites, $FeO.Fe_2O_3$ are actually magnetite, a naturally occurring but technically unimportant ferrite. The additional iron for the divalent Fe^{++} is usually added in the original mix as Fe_2O_3 but then is reduced to FeO or Fe_2O_3 in the sintering or firing process to maintain the 50 % Fe_2O_3 requirement.

Table 5 SATURATION MAGNETISATION OF SOME FERRITES

FERRITES	SATURATION MAGNETOSTRICTION λ_s
$MnFe_2O_4$	-5×10^{-6}
FeF_2O_4	$+41 \times 10^{-6}$
$CoFe_2O_4$	-110×10^{-6}
$Ni_{.8}Fe_{2.2}O_4$	-17×10^{-6}
$Li_{.5}Fe_{2.5}O_4$	-8×10^{-6}
$CuFe_2O_4$	-6×10^{-6}

Guilaud (1957)[2] found that for a fixed Mn concentration , an increase in the Fe content in the initial mix caused the μ versus T slope to be less steep at room temperature . Many Manganese ferrites that contain ferrous ions have a secondary permeability maximum (SPM) , the primary maxima occurring just below Curie temperature .

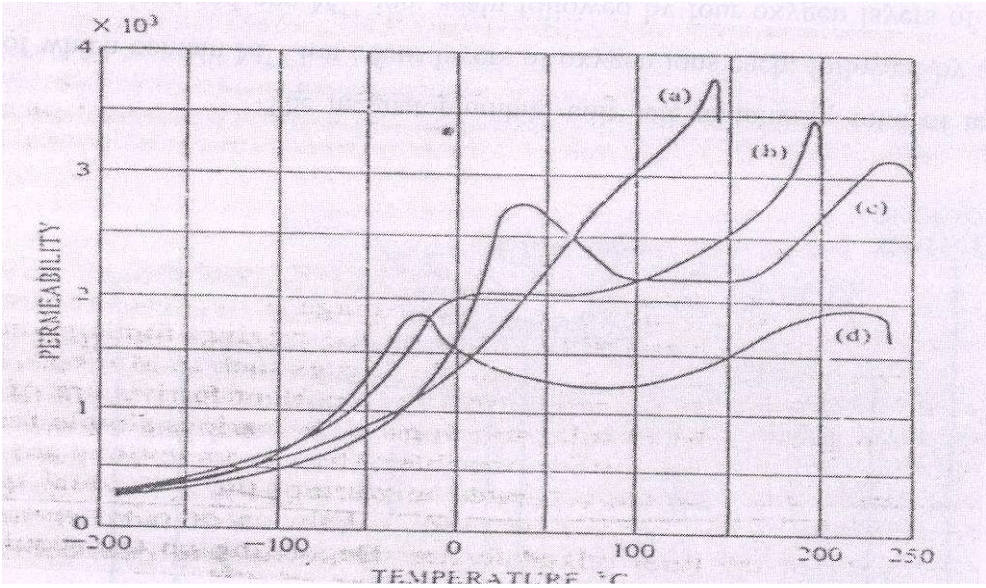

Figure 15 Temp-Permeability Curve for Mn-Zn Ferrites with different Fe contant

As the iron content is increased , the secondary maximum moves to lower temperature. If the highest permeability is desired at room temperature , the iron content is usually choosen so that the secondary permeability maximum occurs at room temperature . This change in temperature dependence of the permeability is due to the movement to lower temperature of point where the magnetostriction goes through zero.

In instances where the permeability maximum does not occur at zero anisotropy , the deviation may be due to the presence of increased porosity which lowers the permeability prematurely as reported by Stuijts, 1964. [3]

2. Ferric Ion Substitution:

Gellio [4] reported in 1958 that ,in some cases , the substitution of other trivalent ions such as Al^{+++}, Ga^{+++}, or cr^{+++} for Fe^{+++} is made for special magnetic or electric functions. These may include reducing the saturation magnetization , increasing the temperature stability , or increasing the resistivity. In the spinal ferrites , the substitution of

nonmagnetic ions such as Al^{3+} on octahedral sites in an inverse spinal such as nickel ferrite will reduce the saturation magnetization since it has net compensated moment.

Gilleo (1958) [4] investigated the substitution of many ions in garnets , his main interest was to reduce the saturation for microwave resonance properties and to increase temperature stability. In the garnets , $Al^{3+}$is often used to reduce the magnetization . however for the garnets, the substitution occurs on the tetrahedral sites which are those that have the uncompensated moments he investigated that when non magnetic ions are substituted for magnetic ions , the curie temperature is reduced , regardless the site where substitution occurs. Divalent ions of metals such as Mn, Fe , and Co can be substituted for Fe^{3+} if equal amounts of quadrivalent Si, or Ge are also added to maintain the equivalent three positive charge of two ferric ions by one divalent and one tetravalent.

3. Effect of divalent ion variation:

In spinal ferrics the divalent ions can be Mn^{2+}, Ni^{2+}, Co^{2+}, Mg^{2+}, Cu^{2+}, Zn^{2+}, and Fe^{2+}. The choice is determined by the specific applications. For materials where large magnetic moments are needed , such as in power applications , the magnetic metal ions with a most unpaired spins are chosen. This is one reason why Mn ($5\mu_B$) ferrite and ferrites that contain uncompensated Fe^{3+}($5\mu_B$) icons are useful. Although Ni^{2+} has alower moment ($2\mu_B$) than Mn^{2+} , $NiFe_2O_4$ has higher resistivity for high-frequency operation and, because of its heiger T_c can function at higher temperature.

4. Permeability dependence on Zinc:

Most commercially important low frequency ferrites contain Zn. Zinc ion substitution for other divalent ion can increase effective magnetic moment. It also contribute in an increase in magnetic permeability . very often, it is the ratio of ZnO to the other divalent oxides as well as the degree of divalent Fe substitution that gives ferrite material developers a greatest latitude in optimizing the properties of a specific ferrite.

In the sintered ferrite the zinc content will depend on the amount that went in originally minus that which was lost in the sintering process. Since Zn is a rather volatile ion , incorrect firing will cause its loss which will lead to a gradient in Zn content

across the thickness of the ferrite. In addition to loosing the chemistry influence of Zn , strains will be introduced , further deteriorating the ferrite.

Zn not only increases the moment , but also lowers magnostriction and anisotropy. The anisotropy of $MnFe_2O_4$ is -28×10^3 ergs / cm^3 . (Bozorth ,1955) [5] and that of $Mn_{0.45}$, $Zn_{0.55}$, Fe_2O_4 is -3.8×10^3 ergs / cm^3 . (Galt, 1951) [6]. In Ni –ferrite , λ_s is reduced from -26×10^{-6} (Smith and Wijn, 1954) [7] to -5×10^{-6} for $Ni_{0.36}$ $Zn_{0.64}$ Fe_2O_4 (Enz,1955) [8]. MnZn ferrites also have so much Fe^{2+} ion that λ_s is usually lower than $1x10^{-6}$

5. Effect of cobalt on permeability:

The effect of cobalt is evidenced primarily on the anisotropy. Co – ferrite or mixed ferrites with co are the only ones that have positive anisotropies . therefore , the anisotropy of the Co-ferrite can be used to compensate the negative anisotropies of other ferrites . Thus , the anisotropy of the mixed ferrite will be zero. Co-ferrite is quite frequently used in Ni or NiZn ferrites for anisotropy compensation .

Both Akashi(1971-71) [9] and Roess(1977) [10] have used cobalt to lower losses and for temperature compensation . Another advantage of cobalt is its ability to make the ferrite susceptible to magnetic annealing .

High frequency losses are also lowered by the addition of Co^{2+}, permitting there use in the high megahertz range. Stijntjes (1971) [11] used co stabilization in combination withTiO_2 in low-loss, low-level applications, whereas Buthker (1982) [12] used Co stabilization in high-power applications.

6. Oxygen Stoichiometry :

Small changes in oxygen content may drastically alter the properties of the ferrite. In some situations non equilibrium atmospheres for the stoichiometric spinel may create conditions for slight oxygen surpluses or deficiencies without the apparent presence of a second phase. These situations occur by the formation of either cation or anion vacancies in the spinel lattice. These vacancies can influence the microstructural aspects by affecting the diffusion rates of the cations.

Tanaka (1975) [13] studied the effects of oxygen nonstoichiometry as well as composition on several magnetic and mechanical properties of MnZn ferrites. Tanaka

looked at how the initial permeability, the frequency and temperature responses of the initial permeability, and the domain structures were influenced by the same oxygen nonstoichimetry. In polycrystalline ferrites fired to grain boundaries, whereas in those fried to give high oxygen parameters, the patterns are random and nuclear.

At lower frequencies, the highest permeabilities are found in the ferrites with low oxygen parameters. The permeability at highest frequency was not dependent on the permeabilities at low frequencies. The permeability is effected by grain size and porosity, but in this case, these effects were minimized by keeping these factors constant.

7. Effect of Foreign Ions on Permeability:

Guillaud (1957) [2] studied the effect of alkali (Na, K) and alkaline earth (Mg, Ca, Ba) impurities on the permeability of MnZn and NiZn ferrites. The impurities were added either by coprecipitating with the original composition or by impregnating the mixture with a salt of the impurity and then decomposing the salt to the oxide. Grain sizes were kept constant. At low impurity concentrations, there is an initial increase in permeability. The steep part of the curve is attributed to the impurity that dissolves in the lattice, whereas the flat portion is the result of saturation and deposition at the grain boundary. The increase in permeability was greater the larger the ionic radius of the impurity, the effect of the ionic radius of the impurity, the effect being great for alkaline earths (+2 valence) than for alkalines (+1 valence). At higher impurity concentrations the effect will reverse and eventually the permeability will decrease due to microstructural effects such as grain size and porosity.

Akashi (1961, 1963,1966) [1] showed that the presence of CaO substantially improved the properties of MnZn ferrites at low concentrations , reached a maximum effectiveness , and then dropped off at higher levels. At still heiger concentrations, Impurities such as SiO_2 create a duplex structure of giant grains with a fine grain matrix which is very derimenntal to permeability..

Many metallic elements such as Mo , V . Cu , Cd and Al show similar behavior, with increases in permeability up to 50 percent at very low concentrations. (Lescroel and Pierrot , 1960) [14]. These materials may initially increase the permeability by acting as sintering aid to increase the density and grain size.

2.4 RECENT TRENDS IN PERMEABILITY OF Mn-Zn FERRITES

I.P.Kilbride and R. Freer [15] prepared Manganese–zinc ferrite ($Mn_{0.52}Zn_{0.41}Fe_{2.07}O_4$) by the mixed-oxide route. Specimens were in the form of toroids, pressed in the green state to 11.9 mm outside diameter and 5.9 mm inside diameter. To assess the effect of zinc loss, they employed, a variety of circular local sintering enclosures. All specimens were initially sintered in air at 1390 C for times of 7.5–16 h. After cooling to 1200 C they were held for 4 h in atmospheres containing 0.0125–0.05% oxygen. Sintered products were single-phase, with density greater than or equal to 95% theoretical and a grain size of about 20 μm. Use of a partial sintering enclosure led them to a 45% increase in initial permeability , but use of a full enclosure led to a reduction in . Firing the samples at 1200 C in an atmosphere containing 0.025% oxygen yielded near-stoichiometric samples, in which the initial permeability was maximized (about 10 200) over a wide range of temperatures 25–90 C.

S.H. Chen, S.C. Chang,[16], reported that the zinc loss will reduce the initial permeability from 11,000 to 6,000. The key sintering parameters increasing this zinc loss are low oxygen atmosphere in high temperature, high gas flow rate in the furnace and the reaction of zinc oxide with Algol. Minimizing zinc loss during sintering is of paramount importance to the successful preparation of high permeability Mn-Zn ferrites.

Beer and Schwarzd [17] have shown that internal stress from Zn loss limits the permeability when growing large grains at high temperatures or for long times. Even though high oxygen content during sintering reduces Zn vaporization, still there are other sources of Zn loss. For example, low partial pressure of oxygen during cooling is the major source of Zn loss. The interaction between saggers and samples is another important source of zn loss'. Re have stressed the effects of oxygen partial preasure, temperature and saggers on Zn loss in this study.

Anjali Verma, Ratnamala Chatterjee [18] prepared mixed manganese-zinc and nickel-zinc ferrites of composition $Mn_{0.2}Ni_{0.8-x}Zn_xFe_2O_4$ (where x = 0.4, 0.5 and 0.6) by the citrate precursor technique. The ferrite powder was obtained on decomposition of the precursor at temperatures as low as 500 ^oC and was investigated for their magnetic and Structural properties such as saturation magnetization, initial permeability, Curie temperature, as a function of sintering temperature and zinc content and properties such as lattice parameter, grain size and density. They reported that mixed compositions exhibited higher saturation magnetizations at sintering temperatures as low as 1200 ^oC. While the Curie temperature decreased with zinc content, the permeability was found to increase. Samples sintered at 1400 ^oC densified to about 94% of the theoretical density and the grain size was of the order of about 1.5 mm for the samples sintered at 1200 ^oC and increased subsequently with sintering temperature.

Manganese-zinc and nickel-zinc ferrites are well-known technological magnetic material. Mn–Zn ferrite is more suitable at low frequencies with their low resistivity and high permeability. In an attempt to increase the versatility of these ferrites for wider range of applications, in the present work, a study of mixed combination of the ferrites was been undertaken, as also to understand the extent of modification of the various properties. Zinc is known to play a decisive role in determining the ferrite properties, hence, the compositional variation in the ferrite was been brought about by varying the zinc content. The redistribution of metal ions over the tetrahedral and octahedral sites in the spinel lattice on incorporation of zinc is responsible for the modification in ferrite properties. The concentration of manganese in the compositions was restricted to 20 mole percent as our previous study on the mixed Mn–Zn ferrite with variations in Mn concentration revealed that ferrites with 20 mole percent Mn exhibited the best magnetic properties. Because the properties of ferrites are sensitive to their composition and microstructure, which in turn are sensitive to their processing variables, the key to obtaining high-performance ferrite is their synthesis by a specialized technique capable of giving compositionally stoichiometric materials. The solid-state method usually adopted for the preparation of ferrites suffers from the disadvantages of prolonged milling to mix the oxides and high processing temperatures resulting in non-stoichiometric compositions. In view of this a solution method known as the citrate precursor method

that is capable of giving atomic-scale mixing of the constituent cations and formation of ferrite powders at low temperatures has been used for the preparation of ferrites in their work .

Li Haihuaa et al. [19] reported that the magnetic properties of Mn–Zn ferrite such as initial permeability, saturation magnetization, Curie temperature, resistivity and power loss are affected greatly by the Fe^{2+} content in the raw materials. The experimental results show that low resistivity (r) and high eddy current loss (P_e) are induced by the superfluous Fe^{2+} content in the raw materials; the scant Fe^{2+} content in the raw materials will increase hysteresis loss (P_h) and decrease Curie temperature (T_c), saturation magnetization (M_s) and initial permeability (μ_i)

In an attempt by Huang Aiping, et al. [20] SnO_2 was added to high-permeability MnZn ferrites and MnZn ferrites for high-frequency power supplies.The effects of the SnO_2 addition were studied. Sn^{4+} ions can dissolve into the spinel lattice and form stable Fe^{2+}–Sn^{4+} pairs which results in compensating the magnetocrystalline anisotropy constant and improves the initial permeability effectively. The initial permeability of ferrites is also improved as abnormal grain growth caused by ion vacancy is controlled with SnO2 doping. In addition, the SnO2 doping also leads to a decrease in the relative loss factor and an increase in density. The power loss and minimum power loss temperature decrease with SnO2 doping.

Setsuo Yamamoto et al. [21] successfully fabricated Mn–Zn ferrite platelet cores with few vacancies using spark-plasma-sintering (SPS) method. Laminated cores composed of Mn–Zn ferrite were prepared. Which shown large saturation magnetic flux densityand high permeability at high frequencies. These soft magnetic cores maybe available as the magnetic cores of a magnetic head used in a card reader or the soft magnetic substrates of the perpendicular recording hard disks.

Debashis Dey and Richard C. Bradt [22] schematically studied the grain growth of ZnO during the liquid-phase sintering of binary ZnO-Bi_20_3 ceramics with **3** to 12 wt% Bi_20_3.

The results were considered in combination with those of their previous studies at lower Bi_20_3 levels. Following a low Bi_20_3 content region where the ZnO grain size is independent of the Bi_20_3 content, the grain size gradually decreases with an increase in the Bi_20_3 content. The kinetic exponent for the ZnO grain growth has been estimated to be 5 and the activation energy and pre-exponential term increased with an increase in the Bi_20_3 content. It has been previously reported that the mechanism of grain growth changes from one of solid-state diffusion of Zn^{2+} cations for the sintering of "pure" ZnO to one of solution precipitation for the liquid-phase sintering in the presence of the liquid-phase-forming Bi_20_3. For the initial additions of Bi_20_3, the ZnO grain-growth rate is controlled by thc solution-precipitation phase-boundary reaction. However, at higher Bi_20_3 contents, the grain growth of ZnO undergoes a transition of the rate-controlling mechanism from that of the phase-boundary reaction to one of diffusion through the liquid phase. These mechanism changes are accompanied by changes in the activation energy for the grain growth of ZnO from about 225 to 150 kJ/mol at low Bi_20_3 levels and finally to 270 kJ/mol at higher Bi_20_3 levels.

For various applications ferrite materials are required with a high permeability and a small variation of the permeability in a temperature range from 0 to 60°C. From a discussion of the theoretical conditions necessary for the occurrence of a high permeability and a flat μ-***T*** curve in MnZn ferrites, H.P Peloschek and David J. Perduijn reported [23] , it clear that these two requirements are controversial, however, by a proper choice of the composition and a correct application of the method of re-oxidation during sintering, a good compromise can be obtained. In the laboratory a permeability variation of less than ***5*** percent has been realized for a permeability level of 7500 in the above temperature range.

S.H. Keluskara et al. [24] reported that nano-particle ferrite having general formulae $Mn_xZn_{1-x}Fe_2O_4$ with x = 0.35 / 0.40 / 0.45 / 0.55 / 0.60/ 0.65 were prepared using nitrilo-triacetate precursor method. Production of fine grain size material at low temperature is the unique feature of this method. Bulk $Mn_xZn_{1-x}Fe_2O_4$ ferrite material produced by sintering nanoparticles at 950 / 1050 / 1150 / 1250 / 1350 ^OC progressively in nitrogen atmosphere showed high values for initial permeability.

The microstructural development and magnetic properties of MnZn ferrites doped with various amounts of CaO and sintered in atmospheres containing various oxygen concentrations were investigated by Andrej Znidarsic and Miha Drofenik [25]. Their results indicate a strong link among the amount of CaO segregated in the grain boundary, the oxygen concentration during sintering, the average grain size, and the magnetic properties of the MnZn ferrites.

Oriano Bottauscioa et al. [26] implied a numerical procedure, based on a mathematical homogenization technique, is applied to investigate the influence of microstructure on the impedance and classical loss behavior versus frequency in soft ferrites. It is found that classical losses result to be mainly affected by grain resistivity and by grain boundary thickness.

Ammad H. Qureshi [27] investigated the effects of hafnia (0.2, 0.4 and 0.6 wt%) along with impurities such as 0.02 wt% SiO2 and 0.04 wt% CaO on the microstructure and magnetic properties of Mn–Zn ferrites. The specimens have been prepared by the conventional mixed oxide method. It has been revealed that the substitution of hafnium into Mn–Zn ferrites enhances the grain growth. Measurements of initial permeability, resistivity and power loss have been related to the microstructure of sintered ferrites in particular to grain size, porosity and grain boundary phases. He reported that optimum properties could be achieved with additive level of 0.4wt% HfO_2 .

Initial Permeability of samples as a function of additives and impurities

HfO_2 (wt%)	Initial permeability			
	No impurities	CaO	SiO_2	CaO/SiO_2
0.2	1064	505	1395	735
0.4	1277	891	1469	1031
0.6	1194	614	1427	866

Hafnia (0.4 wt%) with SiO_2 and CaO enhances density, while the presence of CaO decreases density. The addition of SiO_2 promotes the grain growth, while the addition of

CaO inhibits the grain growth. With simultaneous addition of both impurities (SiO_2–CaO) a balanced microstructure (small and large grains) could be produced.

The initial permeability values are higher for all the compositions having SiO_2. However, combine addition of CaO and SiO_2 decreases the permeability due to the formation of secondary phases at the grain boundaries but the values are higher than CaO–HfO_2 samples.

T. Kasaharaa,et al. [28] studied domain wall motion in Mn–Zn and Ni–Zn ferrites with applied magnetic fields. It is found that Mn–Zn ferrite have a mean grain size of approximately 10 mm and several pores with sizes ranging from 0.2 to 1.1 mm. In situ observations by Lorentz microscopy with an applied magnetic field reveals that in Mn–Zn ferrite, the domain walls move easily across the grain boundary. From in situ observations by electron holography, it is clarified that domain wall pinning at the grain boundary retards a sensitive increase in magnetic flux parallel to the applied field direction, which is considered to result in high hysteresis loss.

K. Ono, S. Fukmnga and **Y** Matsuo [29] studied the effects of mixing a high permeability Mn-Zn ferrite with two different additives simultaneously-MoO_3, (known to promote grain growth) and another oxide having a low melting point, and found that, the pairs MoO_3, V_2O_3, had an effect of speeding up ferrite shrinkage, thereby enabling the sintering of ferrites in a shorter time or at a lower temperature. Similarly coupled with MoO_3, PbO had an effect of increasing the ferrite shrinkage rate, resulting in a higher permeability of the ferrite with an initial-permeability measurement of 25.500.

Fausto Fiorillo [30] reports that understanding and controlling the anisotropy energy and its effects has proved vital to the development of soft magnetic materials and their applications. Indeed, acting on composition and structure and working out specific annealing treatments, a large variety of anisotropy-governed behaviors under DC and AC excitation can be obtained. These were discussed with special problems arising in the characterization of anisotropic soft magnets and a few significant applications. It is stressed how features like J–H loop shape, energy losses, and magnetoresistance effects

can be controlled, in crystalline and amorphous materials, by the methods of induced anisotropy. The high-frequency behavior of these materials can be strongly affected by the anisotropy field via resonant absorption of energy. This calls for tradeoff between the values of permeability and resonance frequency.

The control of magnetic anisotropy in soft magnets, made exploiting compositional effects, preparation methods, and suitable thermomagnetic treatments, can lead to a large variety of DC and AC magnetic behaviors. In this way property tailoring can be achieved and a large number of applications can correspondingly be envisaged. Near zero anisotropy is conducive to the softest DC behavior, but it may adversely affect the high-frequency behavior of the material when resonant effects come into play. This calls for fine tuning of the induced or composition dependent anisotropy, in order to achieve the best tradeoff between maximum permeability and cutoff frequency values.

Miha Drofenik et al [31] investigated the effect of various amounts of liquid phase on microstructure development during sintering and the resulting magnetic permeability of MnZn ferrite (MZF) samples. Results revealed that the microstructure and the final magnetic permeability depend on the thickness of the liquid phase film during sintering. The solution-reprecipitation (S-R) process, which is associated with an intensive microstructure development in MZF, starts when a continuous liquid-phase film of critical thickness δ_o, which wets the MZF grains, is formed. The solid-state sintering that takes place before the formation of the continuous liquid-phase film is essential for the final microstructure of MZF

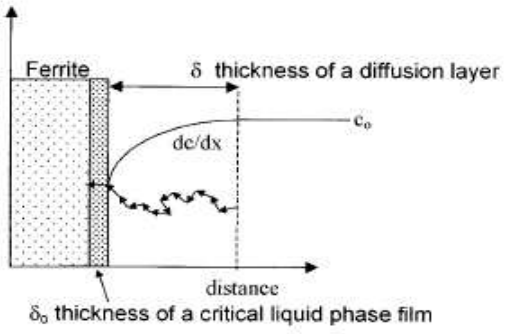

Figure 16: Schematic representation of the condition for the onset of the S-R process associated with a large grain-boundary mobility

The microstructure development and the initial magnetic permeability of MnZn-ferrite cores depend on the thickness of the liquid-phase film during sintering. The essential microstructure elements, the pore-to-pore distance and the average grain size, which govern the free path-length of the domain wall bulging during magnetic polarization, depend on the retarded S-R process. The optimum microstructure of MnZn ferrite, exhibiting the highest initial magnetic permeability, is achieved when the S-R process is retarded and the pore-to-pore distance of entrapped pores does not change significantly when the microstructure changes from inter- to intragranular porosity.

2.5 MICROSTRUCTURAL ASPECTS OF FERRITE'S PERMEABILITY

1. Effect of grain size on Permeability

For obtaining high magnetic permeability the presence of grain boundaries will act as impediment to domain wall motion . the fewer the number of grain boundaries present , the larger the grains and higher the permeability .

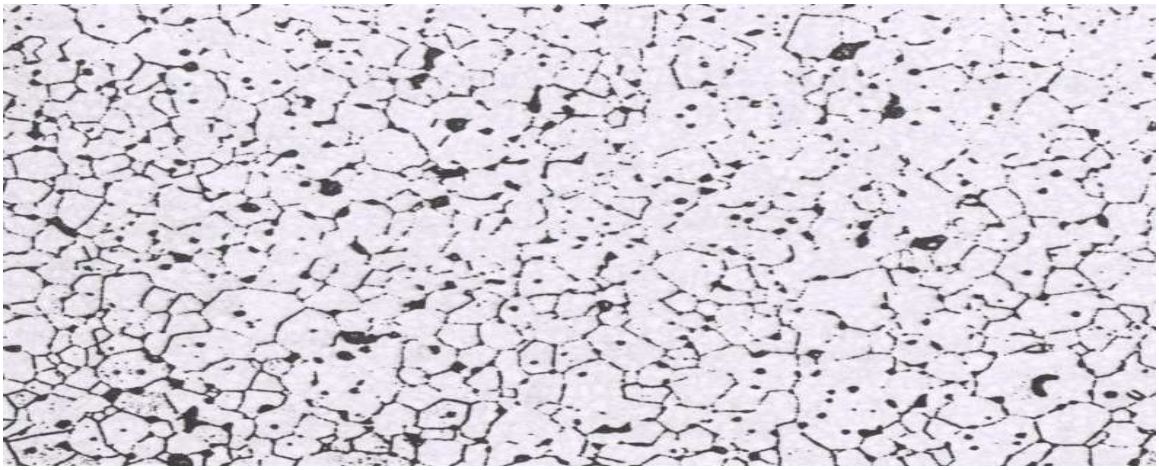

Figure 17: Microstructure of MnZn ferrite (250 X) , permeability = 6000

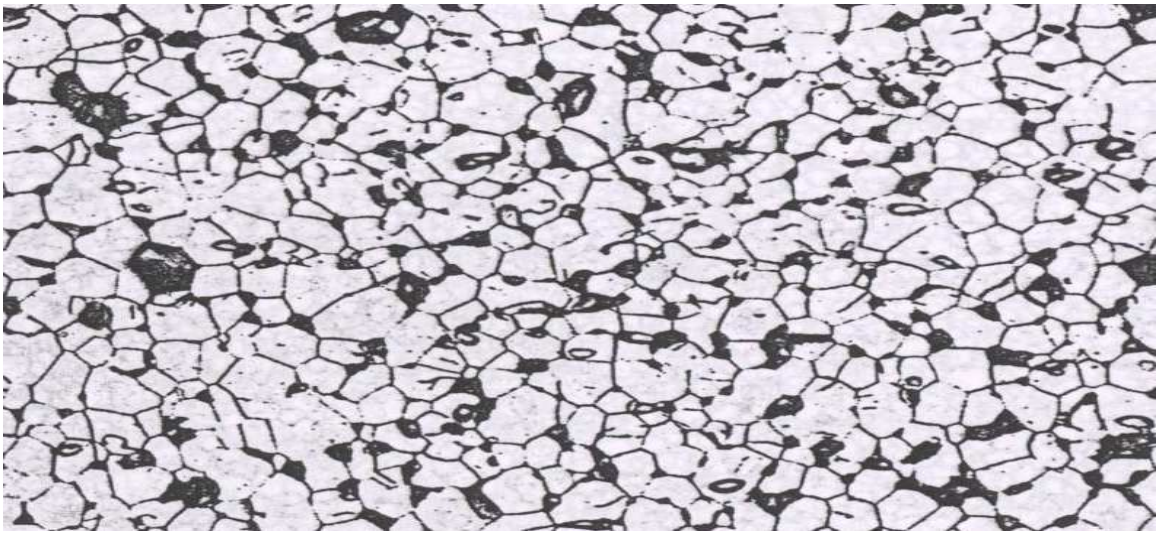

Figure 18: Microstructure of Mnzn ferrite (250 X) , permeability = 10,000

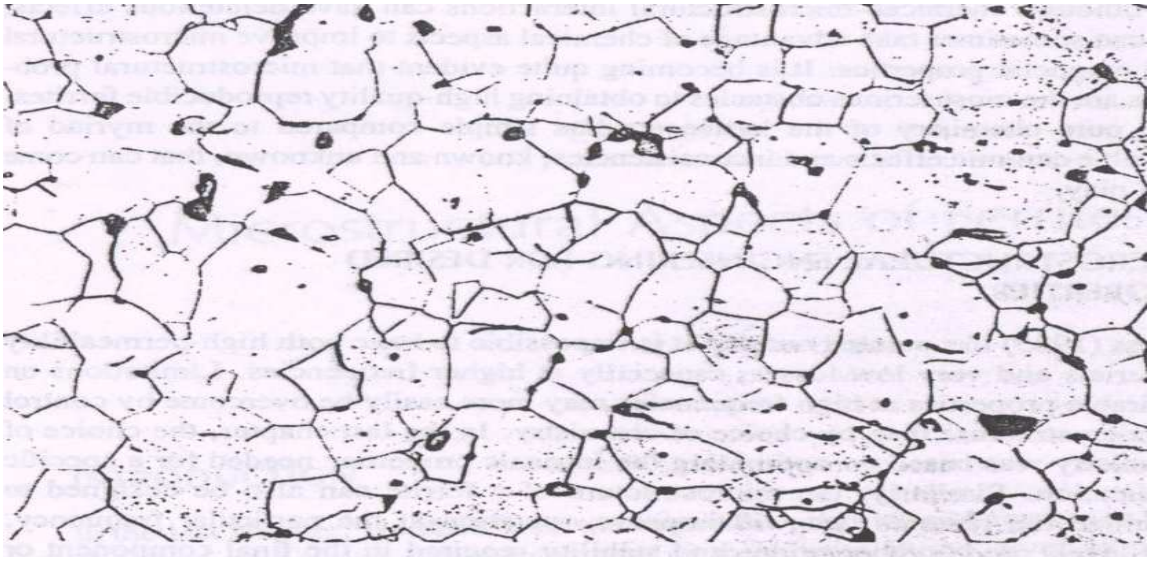

Figure 19: Microstructure of a high-permeability ferrite (250 X), permeability = 16,000

In ferrites where the grain boundaries are thicker , same unhindered movement does not occur. The lack of purification scheme in processing , the presence of pores and inclusions , as well as greater chemical inhomogeneity prevent the attainment of high permeabilities . [32]

2. Exaggerated grain growth in ferrites

The relationship between grain size and permeability will generally be linear only if the grain growth is normal , that, is iff all grains grow pretty much at same time and same rate . this leads to rather narrow range of the final grain sizes. If ,indeed, some grains grew very rapidly they would trap pores , which can limit permeability by pinning domain walls. When conditions permits this kind of grain growth to occur , with many included interagranular pores it is called *exaggerated or discontinuous grain growth.*

Drofenik (1985) [33] has reported that distance between pores rather than grain size account for variations in permeability . samples with gaint grains and included porosity owing to exaggerated grain growth still had higher permeabilities than those with normally grown grains , provided the distance between the pores were the same. Drofenik [33] concluded that the large grained samples are less sensitive to grain boundary effects , and thus the μ versus T curve is more peaked.

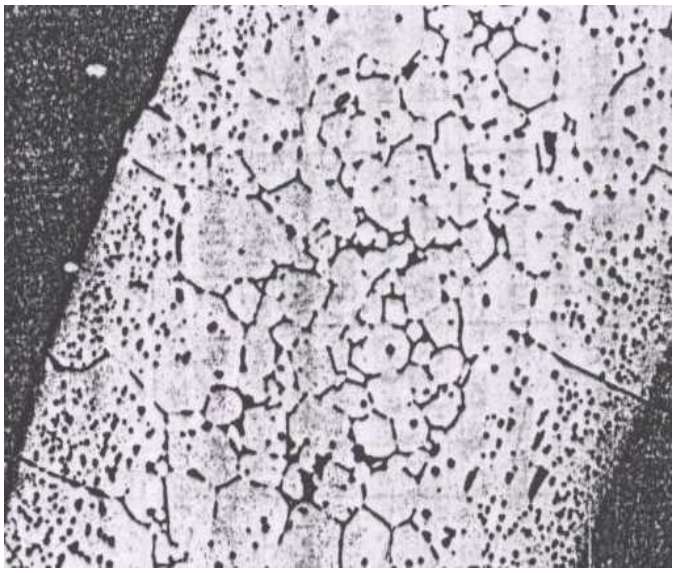

Figure 20: Microstructure of the exaggerated grain growth

Reoess (1971) [34] has reported that the ferrite with exaggerated grain growth and much induced porosity had permeability of 2000, in contrast to the ferrites which grew normally had permeability of 40,000.

3. Duplex grain structure:

It is an undesirable type of microstructure that lowers the permeability and increases the losses. This type of structure has very large grains in the matrix of the fine grains. It is

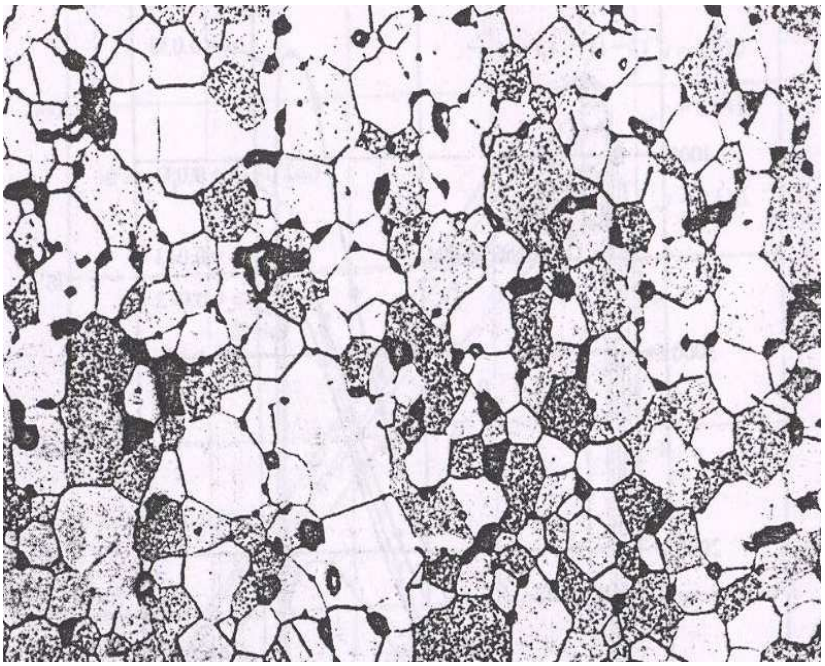

Figure 21: Microstructure of normally grown Mn-Zn ferrite

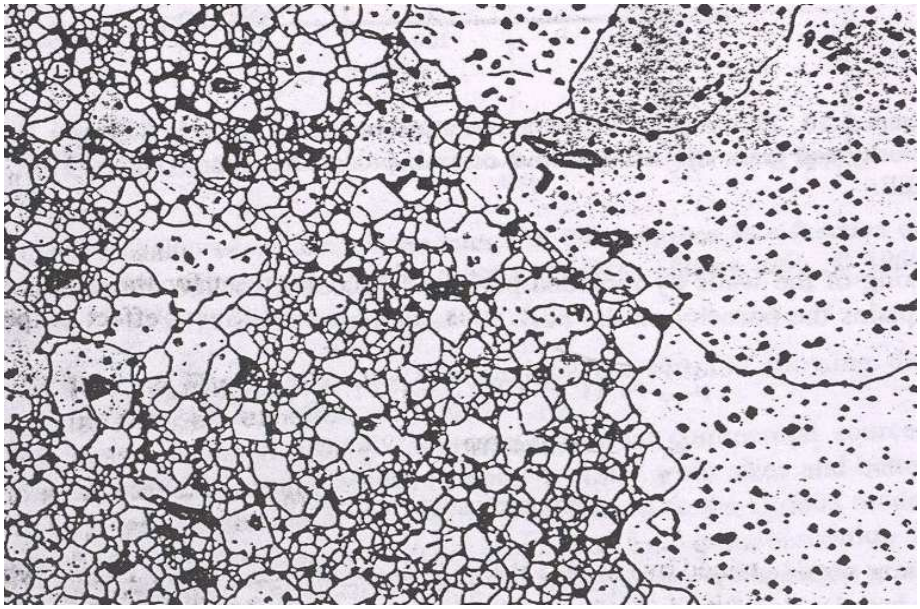

Figure 22: Microstructure of Duplex structure

most often due to the segregation of a particular impurity such as SiO_2 which produces the rapid grain growth locally while other undoped areas are unaffected. (Yoneda, 1980),[35]

4. Effect of porosity on the permeability

porosity is the microstructural feature limiting the movement of domain walls. Pores and other imperfections would appear to pin walls especially within the grain

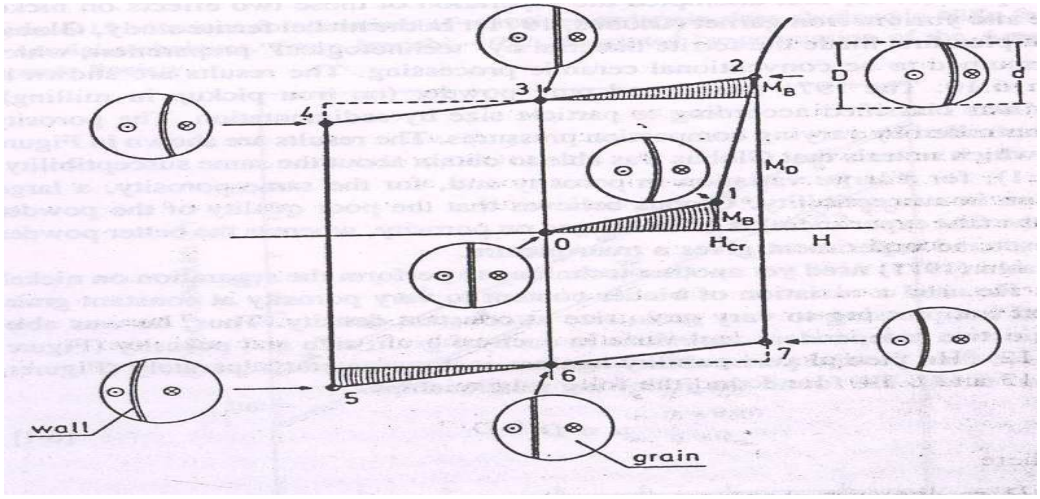

MB = bugling Magnetisation MD = Displacement Magnetisation

Figure 23: magnetization of ferrites showing the domain wall bugling and displacement

Globus (1972)[36] however , point out , domain wall bugling would still permit wall movement even while the end points were tied down. The mechanism illustrated in the figure shows that , the growing of large grains in ferrite creates a problem : many pores are swept over by the grain boundary and remain within the large grains . intragranular porosity is more deleterious than intergranular porosity.

CHAPTER

3

Experimental Work

CHAPTER 3

3.1 FERRITE-PROCESSING

A goal common to all ferrites is the formation of proper crystal structure. The starting materials are conventionally oxides or precursors of oxides of the cations. This process involves the inter-diffusion of various metal ions of a pre-selected composition to form a mixed crystal. Non-conventional powder processing in a liquid medium may produce intermediate, finely divided mixed hydroxides or mixed organic salts to assist the subsequent diffusion process. The whole procedure can be divided into two processing steps:

1. Powder preparation
2. Sintering

(1) Powder Preparation

The ferrite powders were produced by conventional ceramic processing technique, which is one of the most critical steps that control the electrical and magnetic properties of the finally obtained ferrite cores. It consisted of following steps:

1. Dry Mixing

High purity raw materials of the basic composition ferric oxide, manganese oxide and remaining zinc oxide, are mixed and blended homogenously through dry mixing in the pot mill for few hours.

2. Calcination

Homogenously blend of raw material mixture is further exposed to temperature of 950 ^{o} C for 90 minutes in air atmosphere in the batch type furnace. The purpose of calcining is to start the process of forming of spinal ferrite lattice. This process is essentially one of inter-diffusing phenomenon of substituent oxides into a chemically and crystallographically uniform structure. The driving force for the interdiffusion is the

temperature and concentration gradient. As the individual oxides inter-diffuse, some ferrite is created at the interface. This complete phase reduces further diffusion because the concentration gradient is no longer present to act as a driving force. The material in the centre of each oxide particles remains as such, as they experience the difficulty in diffusing through the ferrite since the diffusion distance becomes larger. Since some shrinkage occurs in calcining, one advantage of the process is to reduce the shrinkage in the final sintering. This allows better control of the final dimension of the sintered core. In addition, calcining helps in evaporation of the volatile impurities and homogenization of the powder mixture.

During this process, the powder coarsens considerably, and the color changes from red to grey or black. The degree of calcining action, or in other words spinal formation can be studied from the X-ray Diffraction (XRD) pattern. It shows the peaks of spinal phase formed and the unreacted residual Fe_2O_3 or hematite phase.

Table 6 - Composition of the MnZn ferrite samples

SAMPLE-No.	Fe_2O_3 (mol%)	Mn_2O_3(mol%)	ZnO (mol%)	Bi_2O_3 (wt%)
A	**51.513**	**23.456**	**25.031**	**0.02**
B	**51.614**	**23.862**	**24.524**	**0.02**
C	**52.510**	**24.390**	**23.100**	**0.02**
D	**52.350**	**25.780**	**21.870**	**0.02**
E	**53.020**	**28.180**	**18.810**	**0.02**

3. Milling

After calcining, the material is broken up by ball milling and attrition action. The particle size reduction is carried out to achieve the desired specific surface area (SSA) of 4200 cm^2/gm through ball milling with steel balls followed by fine milling in attritor with 6 mm steel balls. The amount of milling determine the particle size distribution, which in turn influence the homogeneity of the compact going into the final firing as well as the microstructure after the sintering process. In the mid-stage of milling, high purity

additives such as Silica, Calcium oxide, Zirconium oxide etc in desired quantity are added to the slurry in the ball mill. SSA is measured through Blains apparatus.

4. Drying and Granulation

Slurry obtained after milling is then dried in the oven, so as to remove the moisture and obtain a pressable powder. Organic additives such as Polyvenyl Acetate (PVA) and. Polyethylene glycol (PEG) are employed to facilitate this step. PVA is added as a binder to provide adequate green strength to the pressed compact, so that it can be handled easily in the green stage for further processing, PEG acts as a plasticizer so as to soften the particles.The mixture of PVA, PEG and dried slurry is than granulated in the agate mortar, so as to obtain free flowing granulates. The granules are classified by mechanical sieving and the fraction between 200 and 500 µm are subsequently used for pressing.

5. Forming

The next step in the ferrite processing technology is the forming of the components. In this step, dry pressing of granulates into the torroid core configuration is carried out. Dry pressing or compacting is done in a mechanical press using a combined action of top and bottom punches in a cavity such that torroids of external diameter of 29.13 to 29.20 mm, internal diameter of 17.38 to 17.45 mm and height of 14.17 to 14.25 mm is obtained. In this process torroid cores with the green density of 3 to 3.2 gm/mm^3 are obtained.Figure below shows some of the aspects of die pressing.

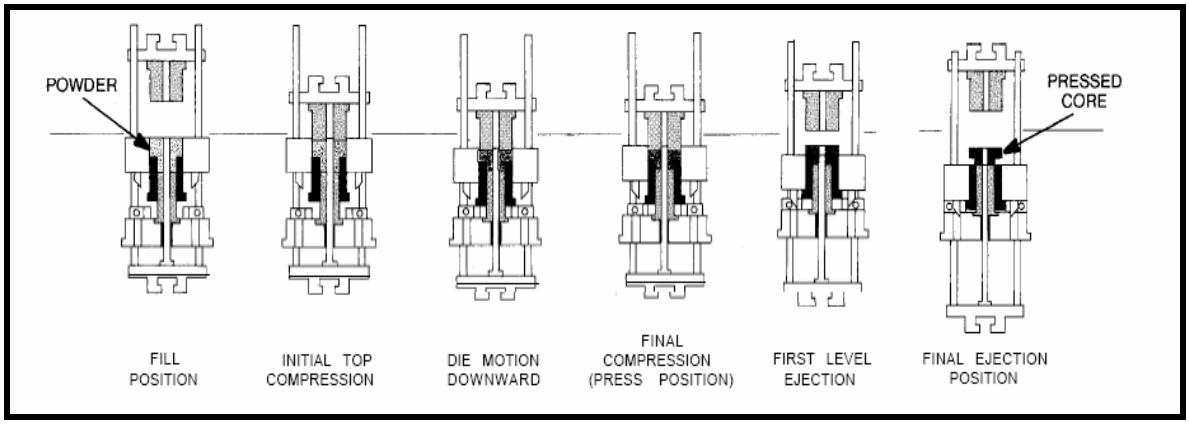

Figure 24: Dry pressing techniques

Before proceeding for dry pressing, granulates are treated with external lubricants such as zinc stearate, which produces a coating of fine lubricant particles on granule surface, as shown in taken from an excerpt from literature**.**

External lubricants also serve to lubricate the die and punch surfaces. The addition of external lubricant increases tool life and helps produce a uniform green body. In addition to providing die-wall lubrication, external lubricants can improve the flow properties of granulated powder by reducing inter-granular friction and hence fill the die more efficiently. Improved packing characteristics can eliminate large

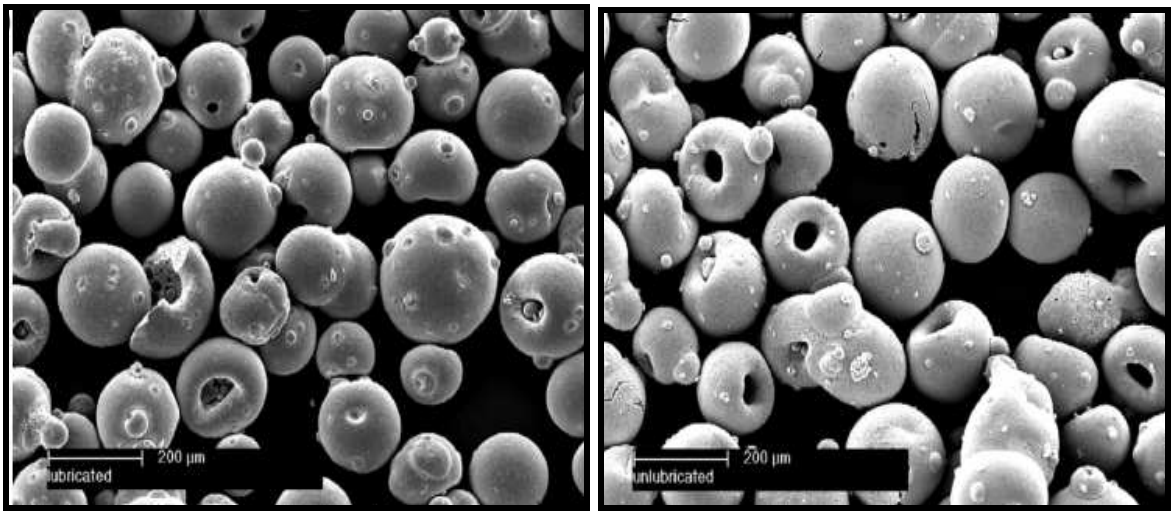

Figure:25 Scanning electron micrographs of granules (a) with external lubricant and (b) without external lubricant.

Inter-granular voids and hence contribute to a low porosity microstructure of the final sintered ferrite core.

(2) Sintering

This is the most critical step in the ferrite processing. It is during this phase of the process that the product achieves its final electric, magnetic and mechanical characteristics. Sintering of manganese-zinc ferrites requires equilibrium between time, temperature and atmosphere along each step of the sintering cycle. Sintering starts with a gradual ramping up from room temperature to approximately 900 ^{o}C as impurities, residual moisture, binders (PVA, PEG), and lubricants (Zinc stearate) are burned out of the product. The atmosphere in this part of the sintering cycle is 20% oxygen (complete air).

The temperature is further increased to the final sinter temperature of 1360 ^{o}C at high heating rate. While the temperature is increasing, nitrogen gas is introduced into the kiln and the partial pressure of oxygen is maintained at 5% at the sintering temperature of the kiln atmosphere. During the cool-down cycle a reduction of oxygen pressure is very critical in obtaining high quality MnZn ferrites and so the oxygen partial pressure is dropped down to ppm level. Sintering of the green torroid samples is carried out in programmable Linn batch kiln. Firing schedules and equilibrium oxygen partial pressure conditions maintained are indicated in the sintering profile**.**

Figure shows the typical sintering profile carried out in this project

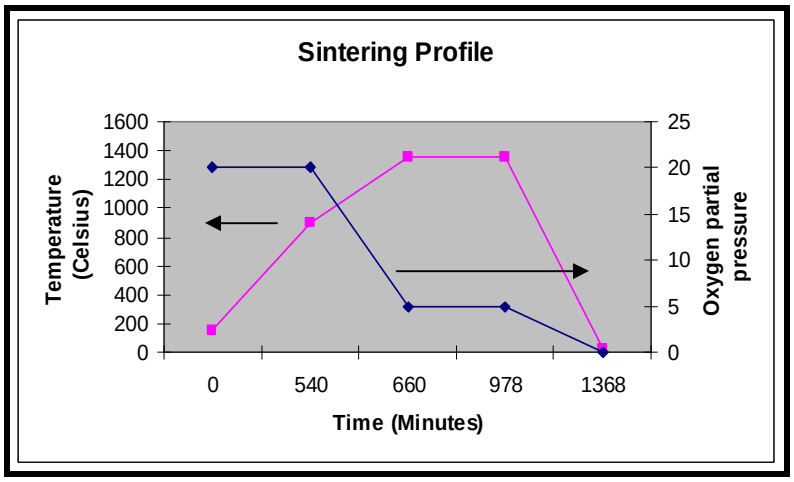

Figure 26: Schematic Diagram of the atmosphere and temperature profiles used during sintering

Table7- Typical sintering Profile

Sintering Profile			
Time Hrs	**Time(Min)**	**Temp(^{o}C)**	**Oxygen (%)**
0	0	150	20
9	540	900	20
11	660	1360	5
15.3	978	1360	5
22.8	1368	25	0.01

3.2 Characterization

Detailed studies of the Magnetic properties of ferrite samples were carried out. Samples were also put to phase analysis and microstructural characterization.

Electrical and Magnetic Characterization

The measurement of Inductance (L_S) of each sintered torroid was carried out using Hewlett Packard multi-frequency LCR meter (model no.-4275A), and other properties such as initial permeability, were derived using the mathematical relations mentioned in the literature..

For measuring the Inductance value, the torroid samples were properly wound with the copper wire with 20 turns and the measurements were carried out using LCR meter at the test conditions of frequency set at 10 KHz and voltage of 0.005 Volts.

Initial permeability (μ_i) of the torroid samples with 20 turns in the coil were calculated using the inductance value in the below mentioned mathematical relation [**25].**

$$\mu_I = [4\pi L_S / h \ln(D_1/D_2)] \quad (1)$$

Where h represents the width of the core, D_1 and D_2 are outer and inner diameters of the torroid core respectively.

Variation of initial permeability with temperature was studied using the Curie set up consisting of a wound ferrite sample dipped in the silicon oil containing flask placed over a heater. The ferrite core is uniformly heated at a constant heating rate and the Inductance value corresponding to the temperature is measured by LCR meter. Initial permeability was calculated according to equation (1) and its value is plotted against

temperature. Due to the limitations of the available apparatus, Curie temperature of the samples was not measured.

Variation in Initial permeability with frequency is measured similarly through LCR meter and plotted.

Microstructural Study

The microstructure of well-ground and polished sintered specimen was studied by optical microscopy using Nikon optical microscope. The samples were etched with Hydrofluoric acid for 2 minutes.

CHAPTER

4

Results and Discussion

CHAPTER 4

RESULTS AND DISCUSSION

The synthesized ferrite powders and sintered ferrite samples were characterized following the procedure mentioned in Chapter-3**.** Before doing instrumental characterization, powders were visually inspected. Spinal powders were dark grayish/blackish in color. When brought nearer to a permanent magnet, they were strongly attracted to the magnet, suggesting ferrite formation. In this chapter, results obtained from the characterizations are discussed

(1) Inductance value and Initial Magnetic Permeability

The prepared compositions of Mn-Zn ferrites were tested for their permeability values, which is shown in table 8 .

Table 8- Inductance value and Initial permeability of the samples

Sample No.	Ls (uH)	μ_i
A	3.437	7072
B	3.423	6819
C	-	7415
D	3.59	6973
E	2.696	5253

Here we see a sudden dip in permeability value for sample no **E** . The reason behind this dip is the decrease in ZnO mol% of the basic composition of prepared sample. As Zinc support divalent Manganese ions to achieve their magnetic moments in the sintered ferrite cores, so in the inadequate mol% of it the permeability decreases. In case of the

composition **C**, ZnO is present in adequate mol%. For samples having higher mol% of it, the stress are generated, as Zinc is volatile, which reduces permeability value in comparison to best composition out of the prepared samples[36].

The permeability spectrum versus sample range is graphically represented as in figure27-

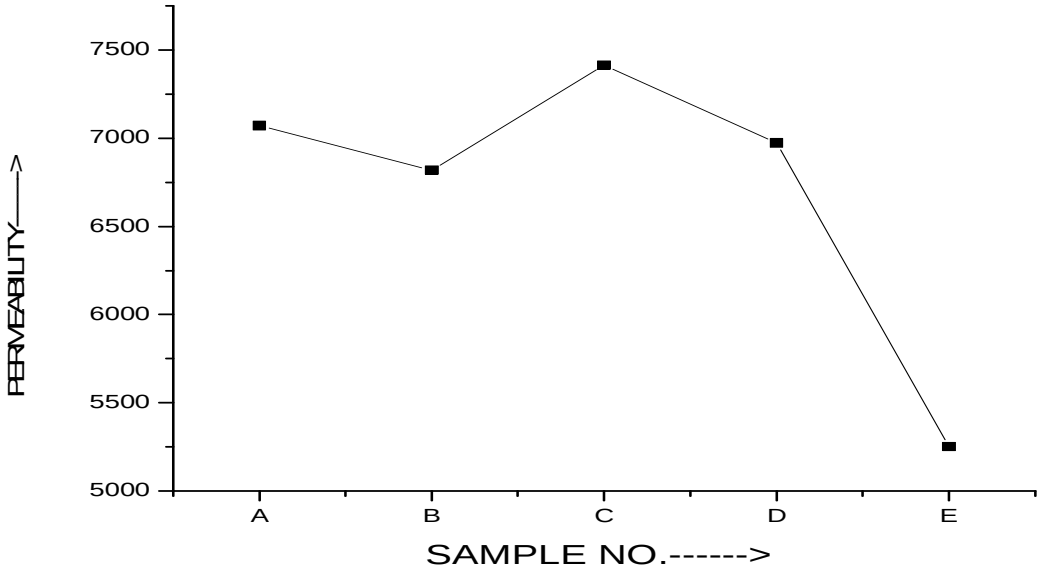

Figure 27: Variation in Permeability versus Sample number

(2) Variation of Permeability with frequency:

The applicability Mn-Zn ferrite samples can be checked by applying a.c. fields**.** The frequency versus permeability graph are shown in figure 28 .The graph indicates that after a particular frequency i.e. approx. 101 kHz, permeability suddenly falls. Therefore, prepared samples are very stable upto 101 kHz. Sample C exhibit higher permeability than other samples because it contain lower porosity. whereas porosity is high in sample E. So its permeability is found to be lowest among all the samples [37].

Table 9: Frequency behavior of Prepared samples

Frequency (kHz)	Sample A	Sample B	Sample C	Sample D	Sample E
10	8874	8820	9114	8139	6236
100	8321	8586	8883	7714	5816
200	5657	6546	7373	6004	4936
400	2456	3073	3242	2643	2455

The frequency behavior of the samples can be explained on the basis of grain boundary pinning effect. Which is more in sample E and least in sample C. Moreover in crystal

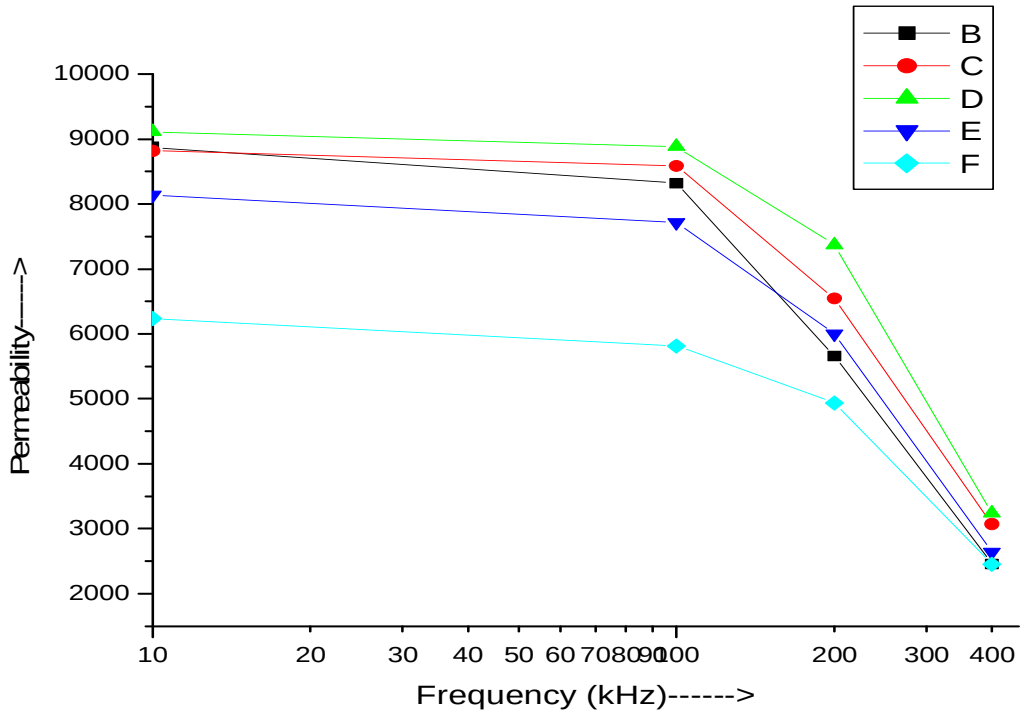

Figure 28 - Variation initial permeability with frequency of the ferrite samples

structure of prepared ferrites, Zn replaces some of the divalent Mn ions, due to which

some uncompensated magnetic moments are left. This is the basic cause of response by prepared ferrites to applied frequency.

(3) Variation in Permeability vs. Temperature:

Permeability is a result of different effects acting simultaneously. Some are inherent properties depending on the chemistry of the crystal structure. Some are extrinsic, depending upon the ceramic microstructure, strains, and so on. With so many factors that are temperature dependent in them, a widely varying curve of permeability versus temperature is obtained.

Table 10 : Variation in permeability of sample A and B with Temperature

Temperature	A(Permeability)	B(Permeability)
28	7072	6819
30	7173	6821
35	7315	7020
40	7597	7227
45	7833	7484
50	8056	7711
55	8358	7944
60	8642	8165
65	8864	8434
70	9235	8785
80	9741	9528
90	8815	9962
96	630	9745
100		6735
102		671

The table gives permeability variation of sample A and B with temperature. It has been observed that the Curie temperature for sample A is 96^0C and that for sample B is 102^0C. whereas the primary maxima is at room temperature.

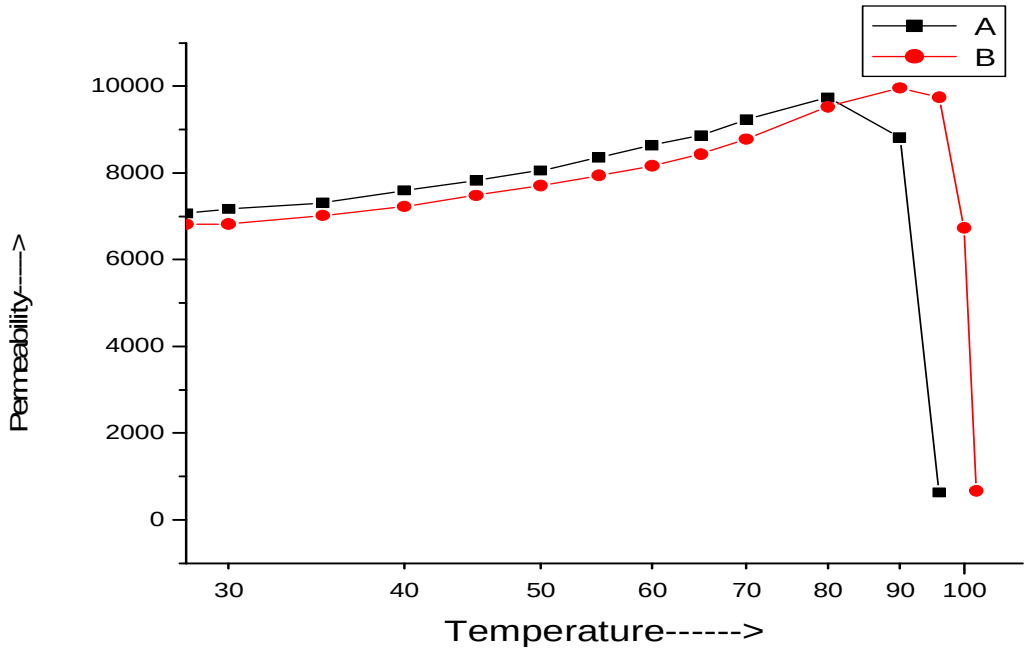

Figure 29- Variation in Inductance with Temperature for selected Mn-Zn ferrite Samples

The best sample out of all five is sample no C. It has been observed that Curie temperature of this sample is 120^0C with maximum permeability.

Table 11 : Variation in Permeability with Temperature for sample C

Temperature	C (Permeability)
24	7415
30	7674
35	7694
40	7721
45	7849
50	7873
55	7912
60	8163
65	8471
70	9027
80	10809
90	12124
100	13167
110	13051
115	12498
120	740
124	0
126	0

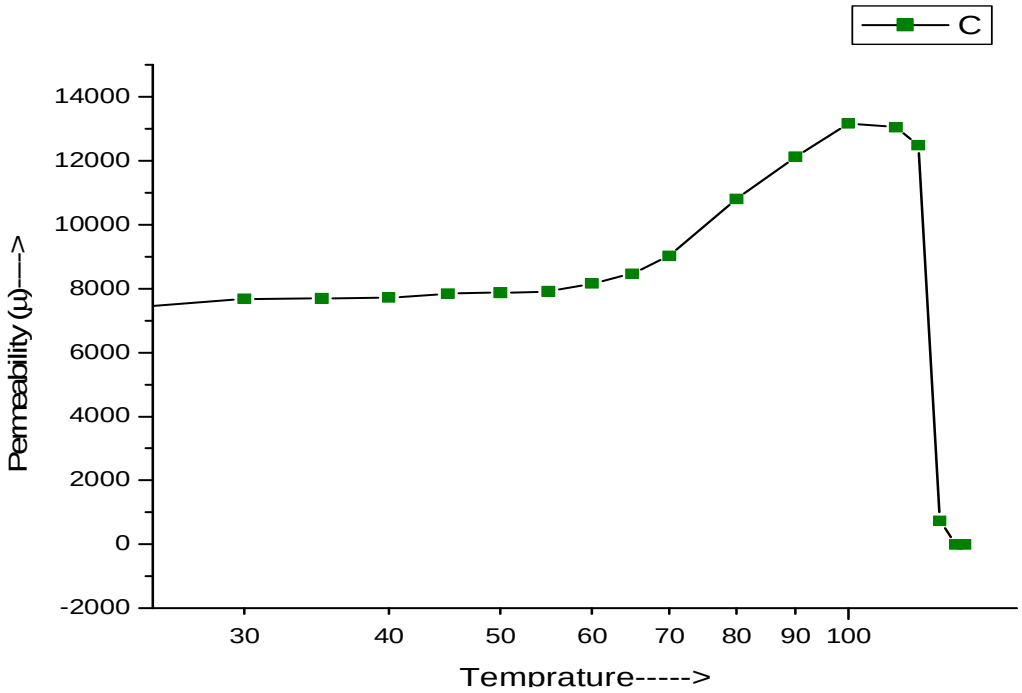

Figure 30- Variation in Inductance with Temperature for selected Mn-Zn ferrite Samples

The increase in Curie point enhances the usability of the ferrites at high temperatures.

Table 12 : Variation in Permeability with Temperature for sample D and E

Temperature	D(Permeability)	E (Permeability)
28	6973	5253
30	7123	5132
35	7062	5023
40	6994	4871
45	6981	4797
50	6981	4688
55	7020	4637
60	7109	4588
65	7231	4571
70	7404	4573
80	7878	4637
90	8612	4793
100	9636	5056
110	11073	5504
120	11909	6110
125	11829	6351
128	10936	6889
132	9588	7289
136	639	7781
140	0	8576
150	0	10038
155	0	10940
160	0	11068
162	0	4312

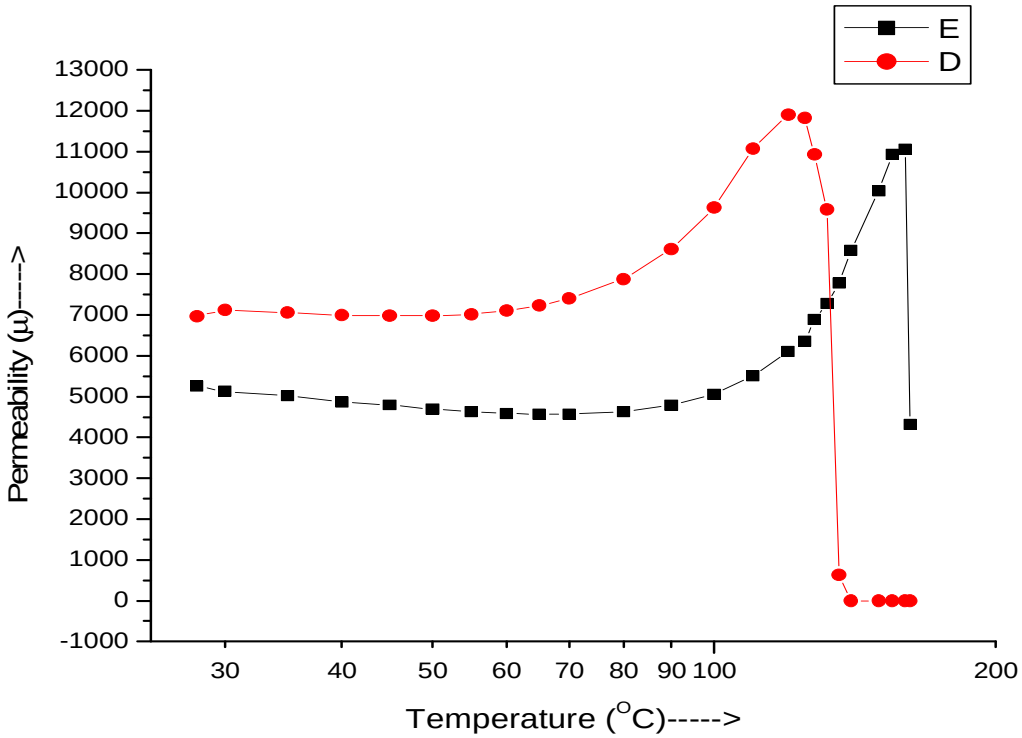

Figure 31- Variation in Inductance with Temperature for selected Mn-Zn ferrite Samples

Similarly the permeability of sample D and E versus temperature are tabulated in table and plotted in figure and their curie temperatures are found to be 136^0C and 162^0C.

(4) Comparison of Curie Temperature:

The Curie temperatures of all the prepared ferrite samples was recorded and is shown in

Table 13 : Comparison of Curie Temperature

Sample No	Curie-Temperature
A	**96**
B	**102**
C	**120**
D	**136**
E	**162**

Table. It shown graphically in figure: 32. With the decrease in ZnO mol% there is increase in Curie temperature this is due to the fact that, with decrease in ZnO for the

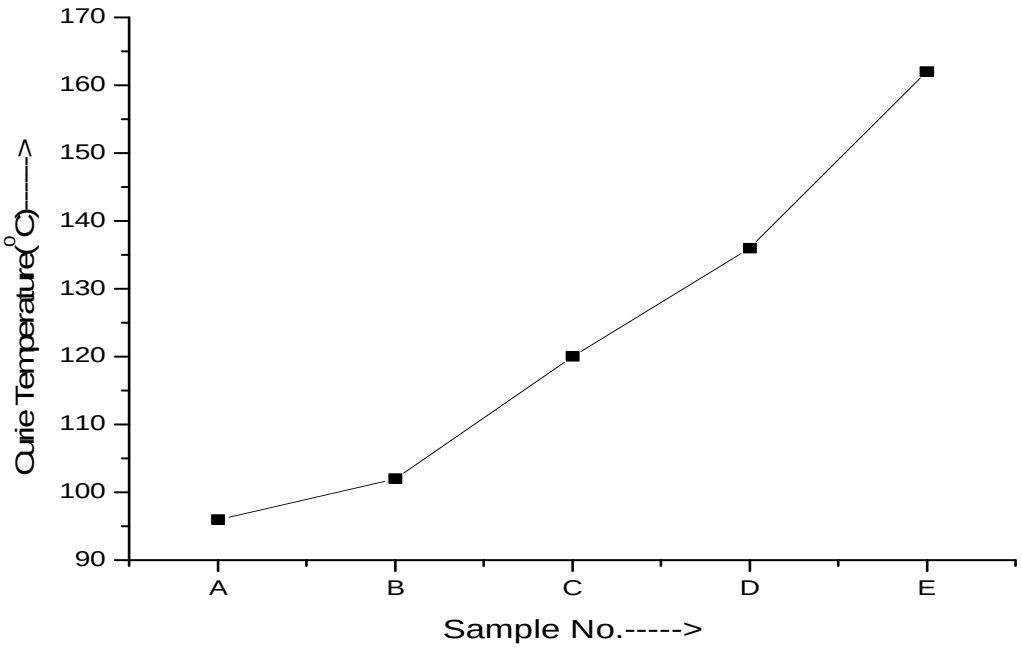

Figure 32: variation of Curie temperature with sample number

compositions there is increase in iron content that is resulting in pronounced increase in curie temperature.

Microstructure Investigation:

Despite of good chemical composition, which is intrinsic property of the ferrite samples, there are some extrinsic properties which can lead to inhomogenieties during final sintering steps. Due to this the variation in properties is observed. Therefore microstructural defects caused by these inhomogenieties can give very valuable information.

Three out of five prepared samples were investigated for microstructural studies.

Microstructure of sample **C** which exhibit best permeability out of the five samples studied is shown in figure 33 at a magnification of 400X.

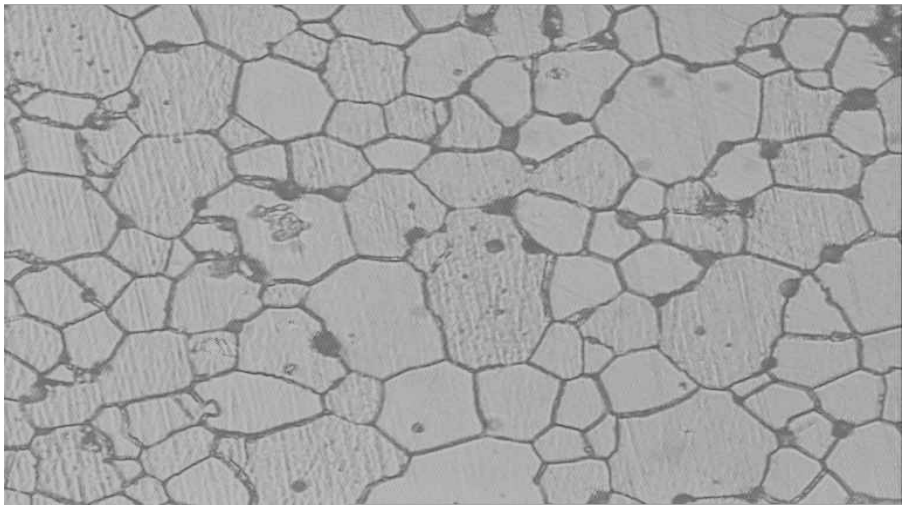

Figure 33 : Microstructure of sample C at 400X

Similarly for sample D the structure obtained at 400X is shown below in figure 34.

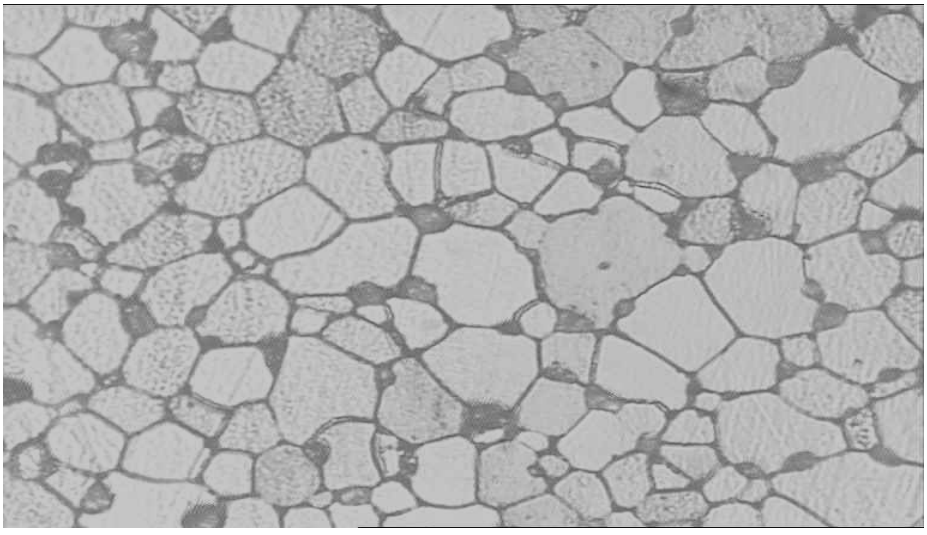

Figure 34: Microstructure of Sample D at 400X

By just visual comparison of figures 33 and 34, we can see the difference in level of porosity in both the samples. For the sample D, porosity is higher as compared to sample C. This is the reason for decrease in permeability for sample D as compared to sample C, as it have lesser grain boundary pinning effect. Similarly Sample E which has lowest

permeability out of prepared samples was studied microscopically and whose micrograph is shown in figure 35 at 400X.

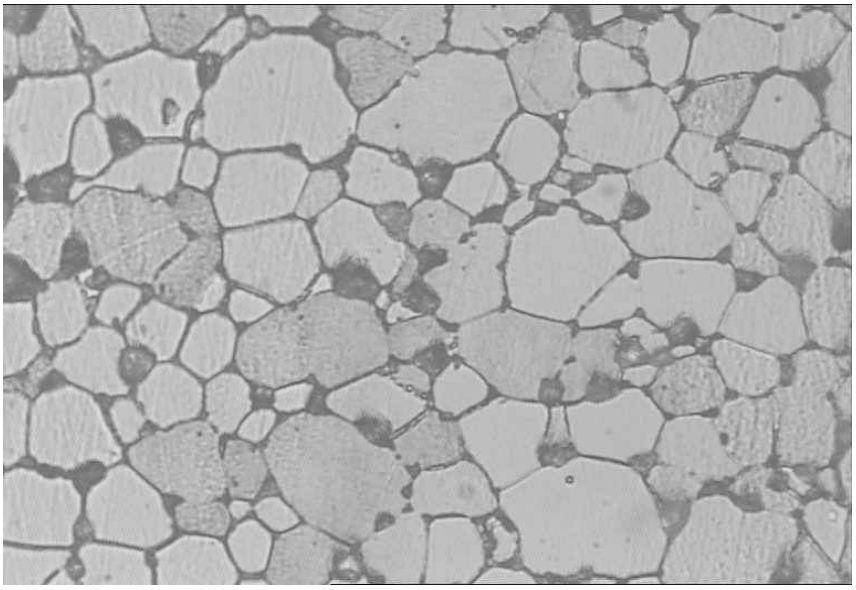

Figure 35 : Microstructure of Sample E at 400X

Here we can see the highest porosity among all the samples, resulting more pronounced grain boundary pinning and have lowest permeability value.

The reason to this porosity is that, as Zn^{++} mol% is decreasing the mismatch between ionic radii of other constituents taking is increasing (for Mn^{++} radii is 0.91 A^0 and for Fe^{+++} it is 0.67 A^0).

The data obtained from Microstructure analysis shown in table 14 below.

Table 14: Comparison of Grain area and %age porosity

Sample No.	Average Grain Area	% Porosity
C	111.635 μm^2	17.72
D	109.53 μm^2	19.86
E	113.682 μm^2	23.09

From this data we can observe that the variation in grain size is not very notable. However, the porosity of samples is showing the variation which is main reason for variation in permeability [38].

CHAPTER

5

Conclusion & Scope of Future Work

CONCLUSION

From the studies of prepared samples it can be concluded that permeability is a very sensitive property, which not only depends upon composition but also on the processing conditions, like sintering temperature etc.

ZnO affects the permeability to greater extent. However, because of its volatile nature it causes defect in the structure.

******

SCOPE OF FUTURE WORK

Mn-Zn Ferrites materials are very promising in the field of switch mode power supplies. Therefore lot more is to be done in this area so that we can have a good response to the applied fields so as to have maximum efficiency out of applied fields.

In order to achieve so, the control of several parameters is to be kept in account, like composition, sintering parameters, purity etc. By controlling these we can achieve better results. With the advent of nano-materials the speculation to increase the quality of ferrite material is getting stronger. As through this we can have better control of microstructure.

All these new techniques are to be taken into account, so that we can have better power supplies in future

******

REFERENCES

[1] Chikazumi, S. 1964. *Physics of Magnetism,* New York: john Wiley & sons.

[2] Guillaud, c. 1957. *Proc. IEEE,* Supp. No: 5, 165.

[3] Stuijts , A.L., et al. *IEEE Trans. Comm. Elect.83.*

[4] Gilleo, M.A. and Geller, S., 1958. *Physics.Rev.110,73.*

[5] Bozorth,et al. A.J.1955. *Phys.Rev.99.*

[6] Galt, et al. F.F. 1951. *Phys.Rev,81,470*

[7] Smithet al. H.P.J. 1954. *Advances in Electronics and Electron Physics6, 69*

[8] Enz,U.1955. *Thesis* , Zurich.

[9] Akashi, T. 1961. *Trans. Jap . Inst. Met . 2, 1963.*

[10] Roess, E. 1977. *J. Magn. And Mag. Mat. 4, 86.*

[11] Stijntjes, T. G. W., P. 1971. *Ferrites, Proc. ICFI, Tokyo: University Press, 191.*

[12] Buthker, et al. T .G. W. 1982 *Ceramic Bull. 61, 809.*

[13] Tanaka, T. 1975 *Jap. J. Appl. Phys.* 1169.

[14] Lescroel, Y., and Pierrot, A . 1960. *Cables and Transmissions 14* , 220.

[15] I. P. Kilbride and R. Freer *IEEE Trans on. Mag., Vol. 36, No. 1, Jan. 2000*

[16] S.H. Chen, S.C. Chang . *IEEE Trans on. Mag., Vol.* 28, no. 5, Sep. 1992.

[17] S.H. Chen, S.C. Chang . *IEEE Trans on. Mag., Vol.* 28, no. 6, Sep. 1993.

[18] Anjali Verma, Ratnamala Chatterjee *Journal of Magnetism and Magnetic Materials February 2006.*

[19] Li Haihua , et al. *Journal of Magnetism and Magnetic Materials May 2001.*

[20] Huang Aiping , et al. *Journal of Magnetism and Magnetic Materials June 2005.*

[21] Setsuo Yamamoto . *Journal of Magnetism and Magnetic Materials 2001.*

[22] Debashis Dey and Richard C. Bradt ***J. Am.*** Ceram. ***S****oc* April , 1992.

[23] H. P. Peloschek and David J. , *IEEE Trans on. Mag.,* Vol No. **3,** *Sep 1968.*

[24] S.H. Keluskar et al. *Journal of Magnetism and Magnetic Materials December 2005.*

[25] Andrej Znidarsic and Miha Drofenik, ***J. Am.*** Ceram. ***S****oc* . *June, 1998.*

[26] Oriano Bottauscio et al. *Journal of Magn. and Mag. Materials Dec 2003.*

[27] Ammad H. Qureshi *Journal of Crystal Growth October 2005.*

[28] T. Kasahara *et al. Journal of Magn. and Mag. Materials August 2005.*

[29] K. Ono, S.Fukmnga and Y Matsuo *IEEE Trans on. Mag.,Vol **35,** No **7, Sep** 1999.*

[30] Fausto Fiorillo . *Journal of Magn. and Mag. Materials* 2006.

[31] Miha Drofenik *J. Am. Ceram. Soc., 86 [9] 1601–604 (2003).*

[32] Alex Goldman, *Modern Ferrite technology.*

[33] Drofenik , *et al. 1985. Advances in Ceramics 16, 229.*

[34] Roess, E. 1285. *Advances in ceramics 15, 38.*

[35] Yoneda, N., 1980. *Ceramic Bull. 59,549.*

[36] Globus, A., 1972 *phys. Stat. solid. 52, 427.*

[37] Hua su,et al. *IEEE Transactions on Magnetics, vol 41, No. 11, Nov 2005.*

[38] Prinya Sainamthip and V.R.W. Amarakoon, *J. Am. Ceram. Soc. 71[8] 644-48 1988*

****
****